CHALMERS
UNIVERSITY OF TECHNOLOGY

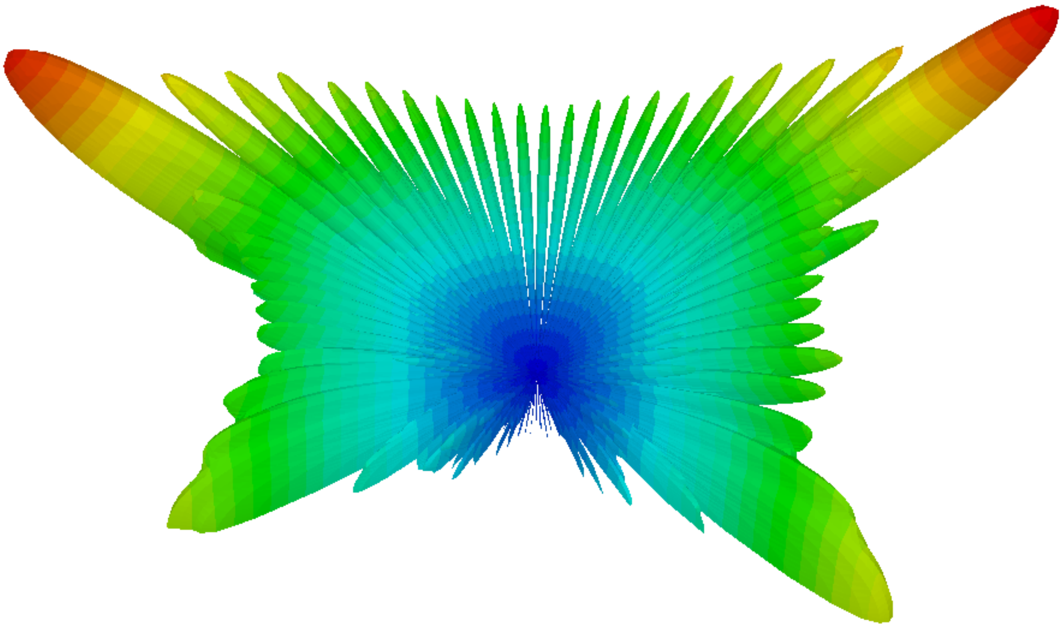

Design of Wide Band, Wide Scan Connected Antenna Array

Master's thesis in Wireless, Photonics and Space Engineering

MIHKEL KARIIS

Department of Electrical Engineering
CHALMERS UNIVERSITY OF TECHNOLOGY
Gothenburg, Sweden 2019

Master's thesis 2019:08

Design of Wide Band, Wide Scan Connected Antenna Array

MIHKEL KARIIS

Department of Electrical Engineering
Antenna Systems Group
Chalmers University of Technology
Gothenburg, Sweden 2019

Design of Wide Band, Wide Scan Connected Antenna Array

MIHKEL KARIIS

Supervisor: Amal Harrabi, Mark Holm, Huawei Gothenburg
Examiner: Jian Yang, Department of Electrical Engineering

Master's Thesis 2019:08
Department of Electrical Engineering
Antenna Systems Group

Chalmers University of Technology
SE-412 96 Gothenburg
Telephone +46 31 772 1000

Cover: Grating lobes of the array with too large element separation

Gothenburg, Sweden 2019

Design of Wide Band, Wide Scan Connected Antenna Array

MIHKEL KARIIS
Department of Electrical Engineering
Chalmers University of Technology

Abstract

The master´s thesis aims to propose a possible solution for the future mobile communications base station antenna. For the 5G standard new frequency bands have been allocated and the spectrum is larger than with previous generations. This means that a wide band antenna should be designed to cover the whole bandwidth effectively, without using multiple narrow band antennas. With 5G comes also the beamforming capability - Massive MIMO, which means that the antenna steers the beam or beams to desired direction. In this way capacity and efficiency can be increased, since power is radiated only towards the user(s) who need it. To cover large area with one antenna the antenna beam should be steerable to high angles from broadside.

In this thesis several planar antennas, feeding methods and balancing networks are investigated and compared for use in the 5G millimetre wave frequency band. A planar dipole antenna array with common mode rejection loop is designed. This broadband antenna array, which is operating in frequency band of 22 to 32 GHz, consists of 484 antenna elements and has a gain of 30 dBi. The designed array has good performance 70 degree in azimuth and 20 degree in elevation scanning in the whole operating band of 23 to 32. The array has a pencil-beam shaped radiation pattern, which is desired in future mobile communication networks.

Keywords: antenna, array, wide band, wide scan, connected array, 5G.

Acknowledgements

I would like to thank my colleagues and especially supervisors Amal Harrabi and Mark Holm at Huawei Gothenburg, with whom I had great discussions and who were of a great help to complete this thesis.

Thanks to all friends and family who were supporting me along the way!

Mihkel Kariis, Gothenburg, August 2019

Contents

List of Abbreviations

ADL	Artificial Dielectric Layer
BALUN	Balanced Unbalanced
CAD	Computer Assisted Design
EBG	Electromagnetic Band-Gap
EM	Electromagnetic
FDTD	Finite-difference Time-domain
FIT	Finite Element Technique
HPBW	Half Power Beam Width
IEEE	Institute of Electrical and Electronics Engineers
MIMO	Multiple In Multiple Out
MoM	Method of Moments
PA	Power Amplifier
PCB	Printed Circuit Board
PEC	Perfect Electric Conductor
SWR	Standing Wave Ratio
UWB	Ultra Wide Band
VSWR	Voltage Standing Wave Ratio

1 Introduction

Array antennas are surrounding us almost everywhere. Most of the routers available today have four or more antennas which work simultaneously. Big radio telescopes around the world are connected to form an array to capture the picture of the black hole, and radars have been using array antennas for long time. This thesis presents the applications of array antennas in future mobile communication networks by stating the advantages challenges and possible solutions to problems encountered today.

1.1 Motivation

More and more everyday devices are connected to internet, kitchen appliances like ovens and refrigerators have built in WiFi connection, bird houses have live video feed to YouTube and internet access is considered as human right. Every day huge amount of data is consumed by mobile users. Higher quality pictures and videos are up- and downloaded by users without realizing the actual size of the data. This however creates need for increased transmission speeds, no one likes to wait hours to upload a short video clip. Higher data rates can be achieved by increasing the bandwidth which in turn is realized by using new higher frequency bands. The purpose of the next generation mobile communication standard, 5G is to provide uninterrupted, high capacity and low latency connection for a wide variety of everyday equipment and devices.

To fulfill the expectations and criteria, set by the standard, new antennas should be developed. Higher frequency, small size and cheap antennas are the key components in this communication network. To meet this demand a solution of low-cost millimeter band antenna should be investigated. In this thesis a connected array antenna, investigation proposed by Huawei Gothenburg, is designed and evaluated to meet these new frequency and bandwidth criteria.

1.2 Goals

The aim of this thesis is to propose a possible solution for cheap, wide band, wide scan millimeter band phased array antenna. This goal is divided into a smaller subgoals which are set as targets along the way to meet the project goal.

One of the subgoals is the design of the unit cell which should be wide band, operating in 23-30 GHz frequency at -10 dB return loss level, and have a planar design. The unit cell should be designed in a way that it would be relatively easy and cheap to manufacture *i.e.* on standard PCB.

Second subgoal is to put the unit cell in the array, calculate array dimensions and determine the geometry of the array.

Finally, the goal for this thesis is to propose a design of a full array, which operates in millimeter wave band from 23 to 30 GHz (30%), has 30 dBi gain, wide scanning angles, beamforming capabilities and planar design.

1.3 Method

To achieve the goals, first existing solutions for wide band antenna arrays are investigated. These antennas are compared and their strengths and weaknesses are noted. From this background information two types of antennas are investigated more thoroughly to decide the appropriate approach to the unit cell design. For that electromagnetic (EM) simulations are made using CST [1]. With help of the simulation results the unit cell is optimized to desired frequency and performance.

When the unit cell has promising performance, it is put into the full antenna array and simulated using CST. Like with unit cell, the array is optimized for wide bandwidth and scanning angles using the results from EM simulations.

1.4 Phased Array Antenna

Antennas consisting of several antennas, which are put together in order to create one large antenna are called arrays antennas. First reports of array antennas are mentioned in [2] but during last decades the usage and studies of array antennas has greatly increased. This is because array antennas have many advantages over single antenna, one of the main being the beam steering capability. By exiting the antenna elements with equal signals, the radiation patterns from single antennas add up and form a pencil beam radiation pattern. However, when the phase of the feeding signals for antenna elements is not equal it is possible to steer the pencil beam to a desired direction. This is advantageous because when having a highly directive antenna, more of the power is concentrated into one narrow spot, which means that the power radiated is higher and therefore range is increased.

Another advantage is the energy efficiency. When having a directive beam, the power radiated is concentrated into one (or many) spots instead of being spread out according to the radiation pattern of a single antenna. Compared to the single antenna higher power output at specific spot is achieved with same input power. Beamforming is one of the key concepts in 5G networks because of the possibility to choose a specific target and communicate with only the desired device

1.5 Connected Phased Array Antenna

Connected antenna array is a relatively new concept and proposes a new approach to solve the common problems like scan blindness and narrow bandwidth in array antennas. Planar structures tend to support surface waves *i.e.* waves, which propagate along the surface of the structure without being radiated. These waves can be unexpected, and it is hard to predict when the surface wave will affect the antenna performance. At certain conditions, like scan angle the surface wave is coupled with the radiated wave in a way that all incoming waves are cancelled, and nothing is radiated. This is called a blind spot in the radiation pattern. These blind spots determine the scan angle of the antenna.

Instead of trying to suppress the surface waves with for example electromagnetic band gap (EBG) substrates in connected antennas the surface waves are uniformly spread out over the surface. With uniform current distribution the impedance along the surface is predictable and therefore a matching section can be designed. With good and wide bandwidth matching section whole antenna will have wide bandwidth and high scanning angle. Concepts and terminology mentioned in this chapter will be more thoroughly explained in next chapter.

1.6 Previous Studies

As mentioned, this concept of connected or coupled antennas is relatively new therefore, there are not so many studies, at least published, about connected arrays. Possibly one of the most extensive studies is done by Daniele Cavallo, who has carried out several studies over a decade. In [3] the concept of connected array is explained with Green Functions, the array prototype is simulated, manufactured and measured. A connected array which achieves 40% bandwidth at VSWR at least 2.1 and scanning angle in elevation of 45° consisting of dipoles is proposed. In relatively recent paper he proposes an alternative design of the array, which is constructed as slot antennas [4]. The bandwidth achieved at VSWR better than 3.5 is *ca.* 85% and scanning angle of 60° in the H-plane and 80° in the E-plane. However, in these studies the frequency band is up to X- or Ku- band and when comparing with similar wide band and wide scan array studies like [5] similar trend is noticed. There are not many, if any, studies, which are addressing the millimeter band for 5G use. Thus, this thesis investigates a possible solution for future mobile communication network which uses 5G technology and spectrum.

1.6.1 Wide band antennas

Wide band antennas have the advantage to cover large frequency bands with single antenna. This is favorable since one antenna is cheaper to manufacture and easier to mount than several antennas. In 5G standard the allocated millimeter wave band is several GHz wide, which is large allocation for communication standard. Today it means that several antennas must be used to cover the whole frequency band, the 4G standard for example uses frequency bands around 700 MHz up to 2600 MHz [6] and by simply scaling the antennas to higher frequency may not provide the desired frequency coverage. Therefore, a new wide band antenna solution must be studied.

There are some wide band antennas currently available, most commonly used might be the Vivaldi antenna [7]. This antenna consists of tapered slot, which follows a specific design function. Most of the times Vivaldi antenna has planar design meaning that the antenna is printed on the PCB, however since the antenna has end fire radiation the circuit board must be aligned respectively. This means that although having a planar structure in design wise the final antenna (array) is not planar and compact. There are some different versions of Vivaldi antenna, like Antipodal- and Balanced Antipodal Vivaldi antenna, but the design and working principle is the same and in performance wise the "regular" Vivaldi antenna shows best performance [8]. However having very wide bandwidth and high scanning range, up to 40 [8] or 60 degrees [9] the drawback is the length of the antenna because the impedance taper should have an electrical length of $\lambda/4$ for good performance, which means that for operation at lower frequencies the antenna becomes too bulky to use as a planar antenna. Connected array antenna provides wide band performance because by connecting the antenna elements the whole aperture is large, supporting the low frequency radiation and on higher frequencies the unit cells which are close together couple higher frequencies.

Taking the previous studies into account the connected array consisting of dipoles shows promising results and therefore in this thesis an array of dipoles for usage in millimeter wave band is designed.

1.7 Scope of the Thesis

This thesis aims to investigate the use of connected arrays in mobile communication equipment *i.e.* in base stations. With 5G standards and new frequency allocation array antennas have good potential for providing mobile network coverage. In future mobile networks the bandwidth is larger than in 4G networks today therefore, wide band antenna would be most optimal in terms of costs and application easiness.

The target frequency range for the antenna dissertated in this thesis is in K-band, more specifically 23-30 GHz, but focusing around 23 GHz. This frequency range is not studied, at least no remarkable papers have been published, extensively and therefore the topic is relevant in order to stay on top of the development of 5G network. When using the IEEE database and searching for ultra-wide band (UWB) or wide scan array every paper which shows up on the top is an antenna or a balun design, which is designed around 8 to 12 GHz. Theoretically the design should be scalable with wavelength but in practice the manufacturing capabilities and later costs are not scalable which means that the antenna design around 23 GHz cannot just be scaled version of the design at lower frequency. Although previous designs are used as a starting point for the antenna design in this thesis.

In general, the antenna design consists of the design of the radiating element, realization the feeding structure, impedance transformation to 50 Ω and a possible BALUN design. All tasks are relatively time consuming and therefore in this work the focus is on the radiating element and a transformer design.

For several reasons mentioned throughout the thesis an array consisting of vertical dipole antennas is designed. First an isolated unit cell is designed using Computer Assisted Design (CAD) software and the performance is verified with EM simulations. After this the unit cell is simulated in presence of other elements in an infinite array and also in finite array. The requirements or guidelines in the design of this array antenna are that the antenna should be wide band and have a wide scan angle, operate in the K band, have a planar design based on commercially available PCB technology and provide a gain of at least 30 dBi.

1.8 Simulation software

In this thesis CST- Computer Simulation Technology [1] by Dassault Systems is used for modelling and simulation. This software was chosen firstly because of availability and user interface, but also because several other papers have used this same software and it good to compare the results when same software is used for the calculations. It is also reported in several comparisons that CST is faster than its rival Ansys HFSS [10], which is advantageous since there is a limited time to perform the simulations and as the simulations show small changes in dimensions have quite significant impact on the performance and many sweeps are made to optimize the dimensions.

Another convenient tool that CST provides is the array task. It is very simple to create both finite and infinite arrays in CST from the unit cell. Also, for same design both time- and frequency domain solvers can be used making the usage faster. A slight drawback however is the lack of EM field solving possibility. In HFSS one can see how the field propagates, making it easy to check impedance mismatches whereas in CST only the magnitude of the field is calculated.

CST uses Finite element technique (FIT) [11] to solve the electromagnetic calculations. By solving the differential equations in time domain CST can calculate wide frequency span with one simulation. Whereas HFSS uses Method of Moments (MoM) which calculates the current or charge density, instead of E or H field, in frequency domain [12]. MoM is reported to be more suitable for frequency sweeps and for radiation problems while FIT, which is based on Finite-difference Time-domain method (FDTD) Since the intention is to design a wide band antenna CST seems to be well suited for this application.

1.9 Ethical aspects

Although dealing with electromagnetics, the scope of this thesis is to design and simulate the work in CAD software and not to do the measurements in real life. There are studies about millimeter band health concerns, which are for example discussed in [13]. Most studies say the millimeter band radiation is non-ionizing and therefore is not harmful to humans, but since the wide usage of these frequency bands is still not common, the antenna radiated power when prototyping and manufacturing should be within the recommended levels. The aim of this thesis is to perform simulations and even when designing the power levels used in the simulations are within the real powers used in antennas today.

2

Theory

In this chapter relevant electromagnetic and antenna theory for understanding the antennas and antenna arrays is explained.

2.1 Electromagnetic theory

Antennas radiate electromagnetic waves and therefore it is necessary to explain the theory about electromagnetic waves to understand why the antenna has certain specifications, like polarization.

2.1.1 Electromagnetic waves

Electromagnetic waves are waves consisting of sinusoidal oscillating electric and magnetic field. These two fields are orthogonal to each other and change in one of them will affect the other field. Electric and magnetic fields are created by fast varying current source. This current source creates electromagnetic radiation which in turn is used to transfer information. A simple way to express these waves is in sinusoidal time varying form [14].

$$\cos(\omega t + \phi) = \Re\left\{e^{j(\omega t+\phi)}\right\}, \tag{2.1}$$

where $\omega = 2\pi f$ is angular frequency, ϕ is phase and t time. Electric and magnetic fields can be expressed as vector functions of time and space.

$$\vec{H}(x,y,z,t) = \Re\left\{\mathbf{H}(x,y,z)e^{j\omega t}\right\} \tag{2.2}$$

and

$$\vec{E}(x,y,z,t) = \Re\left\{\mathbf{E}(x,y,z)e^{j\omega t}\right\}, \tag{2.3}$$

where $\vec{H}$ and $\vec{E}$ are instantaneous magnetic and electric field at time t respectively and $\mathbf{H}$ and $\mathbf{E}$ are time-harmonic magnetic- and electric vector fields.

2.1.2 Polarization

When electromagnetic waves are propagating in space, they are oscillating either on one plane meaning that the E-field, when propagating in $\hat{\mathbf{z}}$ direction, oscillates along Y or X axis making the wave to be linearly polarized. However, when the E-field instead rotates around the axis of propagation direction then the wave is circularly or elliptically polarized. Difference between circular and elliptical polarization is that in circular polarization the E-field has same amplitude around the propagation axis whereas for elliptical the amplitude of the wave varies. This is illustrated in figure 2.1 [15].

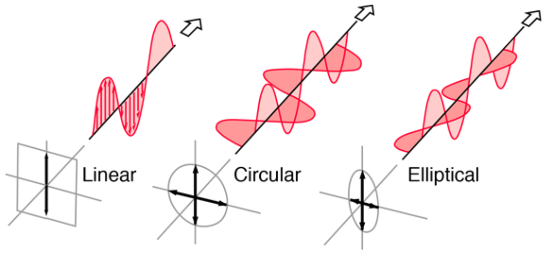

Figure 2.1: Linear-, circular and elliptical polarization [16]

Both transmitting and receiving antennas must have same polarization for good transmission and reception quality meaning that the antennas are oriented at same way. With polarization it is possible to double the capacity of the link by sending in both linear polarization' *i.e.* horizontal and vertical. Ideally the two polarizations are well separated and do not affect each other. However, the advantage with circular polarization is the ability to receive signals no matter the orientation of the receiving antenna. This is advantageous when the receiver is a mobile unit and is not always aligned.

2.1.3 Cross-polarization

As mentioned previously EM waves have a polarization, either linear or circular. When an antenna is designed the polarization is taken into account considering the antenna application. The desired design polarization is called co-polarization. However, when exiting the antenna there will also be an undesired cross- polarization component, which is radiated. Depending of the radiation level this may affect the overall antenna performance and polarization purity. So low cross-polarization level is wanted. Cross polarization ratio is denoted as [14]

$$\mathrm{XP_{dB}} = 10\log\left|\frac{G_{\mathrm{xp}}}{G_{\mathrm{co}}}\right|^2 \mathrm{dB} \tag{2.4}$$

In equation (2.4) $\mathrm{G_{xp}}$ and $\mathrm{G_{co}}$ are the gains of undesired cross- and desired co-polarization respectively and $\mathrm{XP_{dB}}$ is the cross polarization level.

2.2 Antenna theory

Antennas are characterized and compared with each other in several aspects. This is necessary in order to determine which antenna to choose for desired application. Following are the most important and essential parameters which are used for characterizing the antennas.

2.2.1 Far field region

In antenna theory most interesting, at least in the scope of this thesis is the far field region. This is the region where electromagnetic waves radiated by antenna are considered to have planar wave-fronts. Far field region as a distance d when

$$d > \frac{2D^2}{\lambda}, \tag{2.5}$$

where D is maximum length of the antenna side.

2.2.2 Antenna directivity

Isotropic antenna radiates equally in all directions, like a sphere. This antenna would have a directivity of 0 dBi. Such antenna does not exist in real life, but the concept is relevant to compare the antennas. Antenna directivity shows how directive or pointed the antenna radiation pattern *e.g.* beam is. From [17] directivities for some of the most common antennas is noted. The directivity for half wavelength dipole is 2.15 dB, 5-8 dB for microstrip patch and 10-40 dB for highly directive dish antenna.

2.2.3 Antenna gain

Antenna gain is very much related to antenna directivity, but it shows the real radiated power in the maximum radiation pattern direction. This means, that the losses are considered. Antenna gain is measured in dBi which means in decibels compared to isotropic antenna. Antenna gain can be expressed as

$$G = \varepsilon_R D, \tag{2.6}$$

where ε_R is the antenna efficiency and D is directivity.

2.2.4 Antenna efficiency

Antenna efficiency in simple term shows how effective the antenna is in terms of input vs. output power. Efficiency is measured in percentage thus, antenna with 100% efficiency has no losses, all the power sent to an antenna is radiated away. In real life no antenna has efficiency of 1 or 100% because there are ohmic losses caused by materials which the antenna is made of. Typical efficiencies for microstrip patch antennas are above 90% [18].

2.2.5 Bandwidth

Bandwidth is the frequency range in which the antenna is meant to operate or in other words the frequency range where the performance is good. There are several ways to define the *wide* bandwidth depending on the application and frequency range. In this thesis bandwidth is measured at S_{11} -10 dB level and *wide* bandwidth is several GHz. It is also measured in percentage, so called percentage bandwidth

$$BW[\%] = f_{high} - f_{low}/f_c, \tag{2.7}$$

f_{high}, f_{low} and f_c being highest frequency at -10 dB level, lowest frequency at -10 dB level and centre frequency respectively. As mentioned before, this reflection coefficient is set as a goal to stay below in order to not damage the power amplifiers in feeding network.

2.3 Array antennas

Array antennas are, as the name states, antennas consisting of multiple antenna elements, unlike a single antenna, which has one radiating element. Antenna arrays are mostly used because they provide digital beamforming and increased gain compared to single antenna element.

2.3.1 Array factor (AF)

While single radiating element has a radiation pattern, which is dependent only on the radiation characteristics of this one element, array antennas have a radiation pattern which depends on all the elements in an array. For antenna arrays the ***E*** field in far field region is expressed as the ***E*** field of single antenna element multiplied with the array factor [19].

$$\mathbf{E}(\text{ total }) = [\mathbf{E}(\text{ single element at reference point })] \times [\text{ array factor }] \tag{2.8}$$

The array factor is function of the number of elements, geometrical arrangement, spacing and element phases and magnitudes [19]. Array factor is different for every array. When the elements in an array are identical the array factor can be written as

$$\text{AF} = \sum_{n=1}^{N} e^{j(n-1)(kd\cos\theta+\beta)}, \tag{2.9}$$

being the sum of the N elements excitation and phase. It is apparent from eq. (2.8) and (2.9) that by changing the phase and magnitude of the elements the total radiation pattern changes. Therefore, it is possible to steer the beam electronically.

2.3.2 Array gain

Array gain is dependent on the number of elements in the array and the gain of a single element. As a rule of thumb by doubling the number of elements in an array the gain increases by 3 dB yielding

$$G_{\text{array}}[dBi] = G_{\text{single cell}}[dBi] + X \cdot 3[dB], \tag{2.10}$$

where

$$X = log_2(N). \tag{2.11}$$

N being the number of elements in the array.

Maximum array aperture broadside gain can be calculated from [20].

$$G_{Array} = 4\pi\frac{A\eta}{\lambda^2}. \tag{2.12}$$

A is aperture area and η is aperture efficiency.

2.3.3 Beamforming

Beamforming is the key feature of almost all array antennas. One single antenna might have quite wide radiation pattern and half power beamwidth, cell-tower antennas for example have HPBW of 120° [21]. This means that at ± 60° from broadside the main lobe radiates at half of the maximum power. With an array however the radiation patterns from the antennas add up and produce one narrow beam. This beam has high gain, because it is directive and power is concentrated at one spot. This is the feature which is more and more used in modern communication systems. With directive beam a specific user can be selected who needs most power at this instant time. Highly directive antenna has higher range compared to wide beam and it is more energy efficient since power is only radiated at the directions it is needed.

With phased array antennas, it is possible to electronically steer the beam to the desired direction. This means that for example in cell tower the antenna does not have to physically rotate to select target user and in satellite communication the beam can be locked to specific satellite even when either the satellite or station on the ground moves. To realize the digital beamsteering phase difference in input signal should be introduced. Usually the phase difference is linear *i.e.* first antenna has a phase of 0°, second one 10°, third 20° *etc.* Equation (2.13) is used to calculate the phase difference for wanted beam angle from broadside.

$$\Delta\varphi = \frac{360° \cdot d \cdot \sin\Theta}{\lambda}, \tag{2.13}$$

where $\Delta\varphi$ is the phase difference, d is the distance between antenna elements, and Θ is the desired angle. This is illustrated in figure 2.2 where the 45° lines from antennas show the desired beam direction from broadside, also marked with angle Θ. In more complicated antennas beam can be steered in both elevation and azimuth.

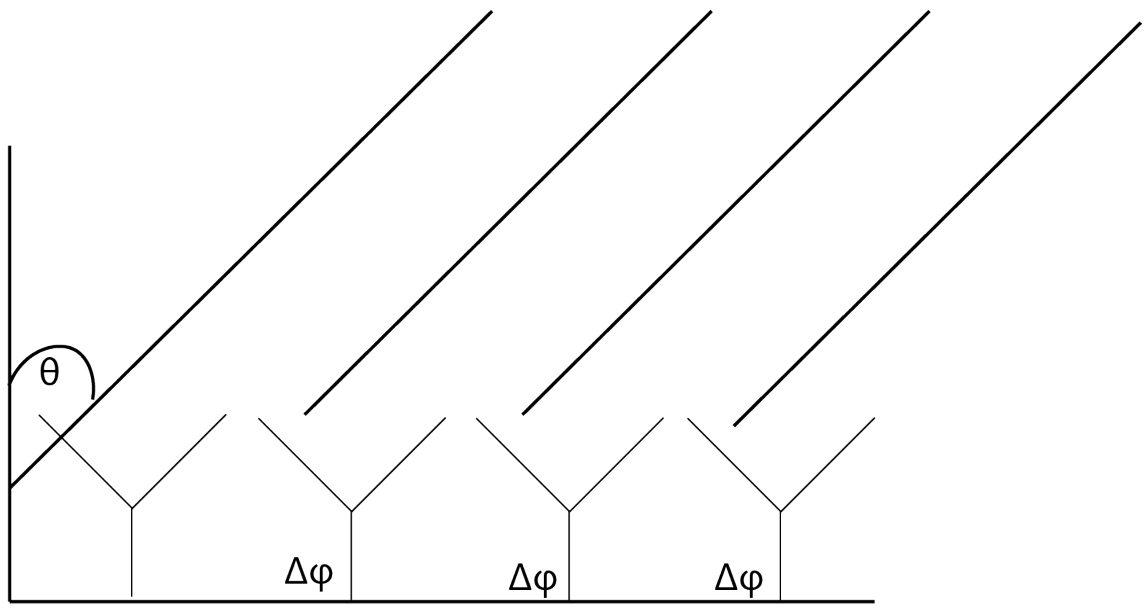

Figure 2.2: Phase difference for beamsteering

2.3.4 Grating lobes

When several antennas are exited together their radiation patterns sum to form a main lobe with high gain. However, when the element separation is too big there will be undesired equally high gain sidelobes *i.e.* grating lobes. These appear in periodic arrays *e.g.* in the arrays where the separation between the elements is uniform. To avoid the grating lobes separation must be

$$d_a \leq \frac{\lambda}{1 + |\cos \alpha_0| + (\lambda/L)}, \tag{2.14}$$

where L is the length of the array, and α_0 is main beam direction, for example 90° for broadside arrays [14]. From (2.14) the separation between elements for broadside array should be up to one wavelength.

2.3.5 Mutual Coupling

In an array several antennas are close to each other, which means that the performance of the one single antenna might be significantly different when in presence of other antennas in an array.

Mutual coupling is an electromagnetic interaction between two or more nearby antennas. Even when antennas are transmitting, they receive at the same time. This means that part of the transmitted energy by antenna is received by nearby antenna [22]. Similarly, when antennas are receiving part of the incident wave is reflected and radiated by antenna. The radiation characteristics of one antenna then does not only depend on the properties and excitation of this antenna but also contributions from nearby antennas. In array antennas mutual coupling is inversely proportional to the distance between antenna elements [23]. Mutual coupling is also caused by surface waves which travel along the surface of the antenna array. To suppress the surface waves and reduce mutual coupling, electromagnetic bandgap (EBG) structures can be used between the antenna elements.

Mutual coupling changes the antenna radiation pattern, affects gain and efficiency of the antenna, causes high sidelobes and scan blindness[24, 25] especially when the array is scanning at high angles. In array antennas coupling is different for different antenna elements, depending on their position in the array. Elements in the middle of the array are affected by coupling in one way and elements at the edges on another way. It is common to model the mutual coupling as mutual impedance of an antenna element instead [22].

2.3.6 Mutual Impedance

When two or more antennas are near to each other the impedance of the one antenna element is different, compared to the isolated elements self-impedance, because of mutual coupling there is an additional impedance introduced to the antenna. In scanning antenna array the impedance of the antenna elements changes during the beam scanning range. This means that the antenna elements must be matched for whole scanning range. This is difficult to achieve and therefore the scanning range is limited, since matching seldom can be achieved over wide band. With coupling, power received from nearby antenna element together with radiated power creates standing wave. High standing wave ratio (SWR) means that there is much power reflected back into the feeding network. With SWR > 2 amplifier in feeding network loses its gain, might become unstable and oscillate or break.

Caused by mutual impedance the driving (or active) impedance, which here is the impedance of one antenna element when all the elements are exited, changes depending on the excitation and the element position in the array. For each element impedance matching for optimal performance is different. Therefore, it is crucial to design a wide band matching network.

2.3.7 Surface Waves

Surface waves are waves which travel along the surface of a material, for example antenna array. They arise on the substrates which $\epsilon_r > 1$ [26]. These waves are bonded to the interface, the higher the frequency the more tightly the waves are bonded to the surface. Surface waves are nonuniform, because the field varies, by exponentially decaying, in the direction perpendicular to the travelling direction. In microstrip antennas the wave is reflected between the dielectric-ground and dielectric-air interface until reaching the edge of the antenna array. The surface wave is refracted on the edge and causes end-fire radiation which furthermore affects the desired radiation pattern.

2.3.8 Scan blindness

Scan blindness is an undesired phenomenon in scanning antenna arrays at which there is no gain at specific angle from broadside or in other means, reflection from the antenna is infinite [27]. This effect is caused by mutual coupling with surface waves and high impedance mismatch when scanning. At certain scan angle the radiated fields from elements add in phase, which changes the impedance significantly therefore increasing reflections [14]. According to [27] the scan blindness occurs when the propagation constant β of radiated wave equals the propagation constant of surface wave β_{sw}. From observations in [27] the blind spot exists when $\beta_{sw}/k_0 \geq 1$. When this ratio increases the blind spot moves towards broadside.

With large ($d_a > 0.5\lambda$) separation between array elements the scan blindness is caused by the grating lobe. According to [14] first radiating grating lobe is at

$$|cos\ \alpha_0| = (\lambda/d_a) - 1, \tag{2.15}$$

where d_a is the separation between the antennas and α_0 is the angle from array surface, towards normal. From equation (2.15) it is apparent that the radiating grating lobe is not present when $d_a < \lambda/2$ because $|cos\ \alpha_0| > 1$ [14].

Another cause for scan blindness, as briefly mentioned before, is the presence of surface waves. From [14] scan blindness is at an angle when

$$k|cos\ \alpha_0| - \frac{2\pi}{d_a} = -k_{sw}, \tag{2.16}$$

where k is the wavenumber of radiating wave and k_{sw} wavenumber of the surface wave. At this angle surface wave acts as a non-radiating grating lobe but since it propagates along the surface of the array it couples the antenna elements and thus may change the impedance rapidly.

2.3.8.1 Eliminating scan blindness

There are many proposed approaches in literature to reduce or eliminate blind spots in the scanning plane. Most studies propose the suppression of the surface wave, since the coupling due to surface wave Floquet mode is the cause of impedance mismatch and blind spot.

In [28] electromagnetic band-gap substrate is proposed. With EBG the gap is designed for the operating frequency and therefore the propagation of surface waves is not supported. However the main disadvantage with this method is that the achieved bandwidth is relatively narrow for wide band arrays, about 4.9% at -10 dB. In this thesis wideband *e.g.* scan blindness problem is looked from mutual coupling point of view by increasing the coupling.

2.3.8.2 Benefits of mutual coupling

Although having many negative effects it is becoming more and more common to intentionally increase the coupling between the antennas in an array. In [3] connected array of dipoles is proposed. By moving the antennas close to each other and connecting them together, the array can be seen as single antenna with constant current across the whole array surface. When antenna elements are closer together the capacitance between them increases. In simple terms the capacitance between the antenna elements together with the ground plane inductance creates high frequency resonating LC circuits. Thanks to that connected arrays achieve wideband performance. Another advantage of connected arrays is the wide scanning range. The array has low cross polarization even at high scan angles. When antenna elements are closely coupled the current along the surface is more uniform and so is the impedance. When having a known and predictable impedance of the antenna it is possible to design a wideband matching network.

2.3.9 Connected array

Connected array is a different approach to try to increase the antenna bandwidth and scanning angle. The term connected comes from the fact that the antenna elements in the array are either very close to each other, connected through the ground of physically connected as in [3], where two unit cells consisting of planar dipoles are connected so that the arms touch. In connected array the whole antenna array can be seen as one single wide band antenna, instead of multiple antenna elements. The antenna elements in the connected array have separations that are smaller than $\lambda/2$.

3

Patch antenna design

In this chapter a patch antenna is designed to introduce the basics of antenna design and feeding but also since the patch antenna has a planar design and might be suitable for the array. First a single patch antenna is designed and different feeding methods in terms of antenna bandwidth and HPBW are compared. Then an array with several patch antenna elements is designed and the coupling effects are discussed.

3.1 Single patch antenna

For understanding the problems with connected arrays and have some insight about the design and feeding, a most simple planar single patch antenna is designed. To find the initial dimensions for the patch at f_c=28 GHz online calculator [29] was used. The dimensions of the patch were optimized in CST to get as low S_{11} at desired frequency as possible. The size for the patch is W=3 mm, L= 2.62 mm, h_{patch}= 0.035 mm, RO4003C 0.203 mm substrate with permittivity of 3.55. Patch is fed with 50 Ω Teflon (ϵ_r= 2.55) coaxial cable with inner diameter of 0.185 mm and outer diameter of 0.7 mm. Feed position is taken 1/6 of patch width away out from the center. These values yield far field pattern and S_{11} as in figure 3.2. The maximum gain is 7.25 dBi and 3 dB beamwidth 82.3°.

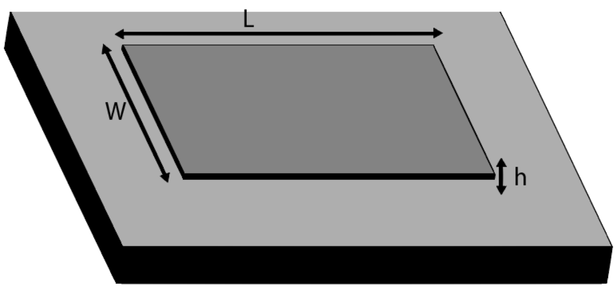

Figure 3.1: Geometry of the single patch on top of dielectric

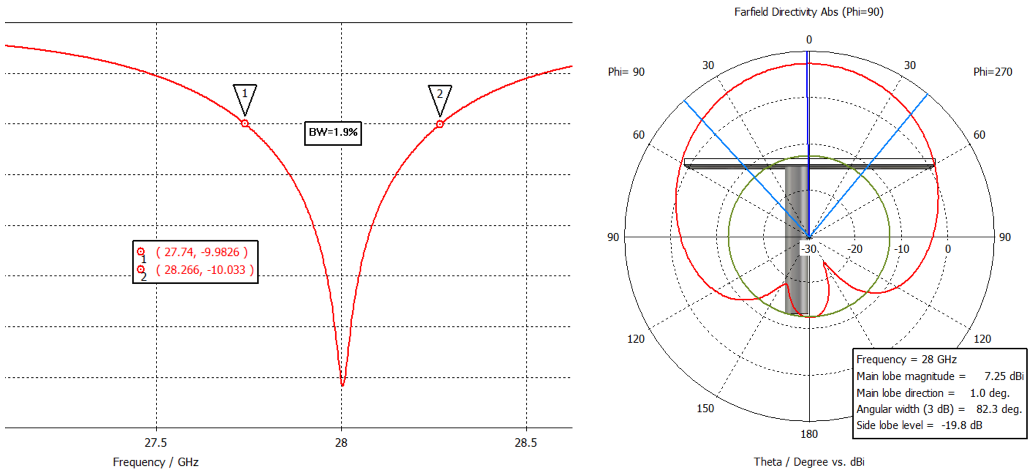

Figure 3.2: S11 of single patch antenna (left) and Farfield pattern of the patch (right)

3.2 Array of two patches

The performance of one patch is compared with an array consisting of two patches. The radiating elements are $\lambda/2$ apart from each other. Far field pattern is plotted in figure 3.3. The antenna gain is 10.7 dBi and 3 dB beamwidth 34.4° and 84.1° for Theta cut, Phi angle of 0 and 90 degree respectively.

Bandwidth is the same as for single patch antenna, about 1.9% but the resonance frequency is slightly lower than for single patch. This is due to the coupling, which makes the radiating element slightly bigger and therefore resonance frequency is shifted downwards. The coupling between two antenna elements is bit less than -20 dB.

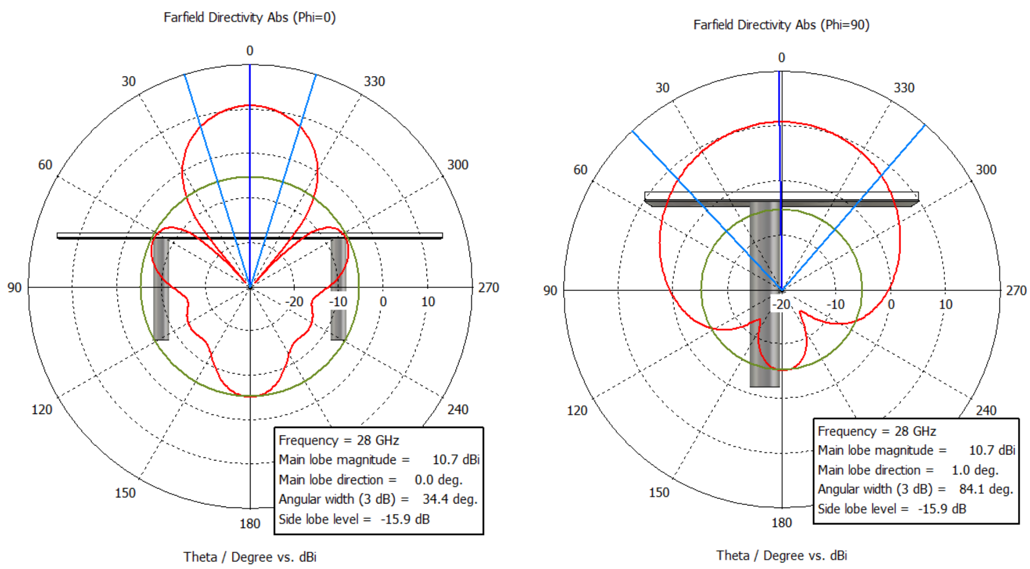

Figure 3.3: Farfield pattern for the two-patch antenna array

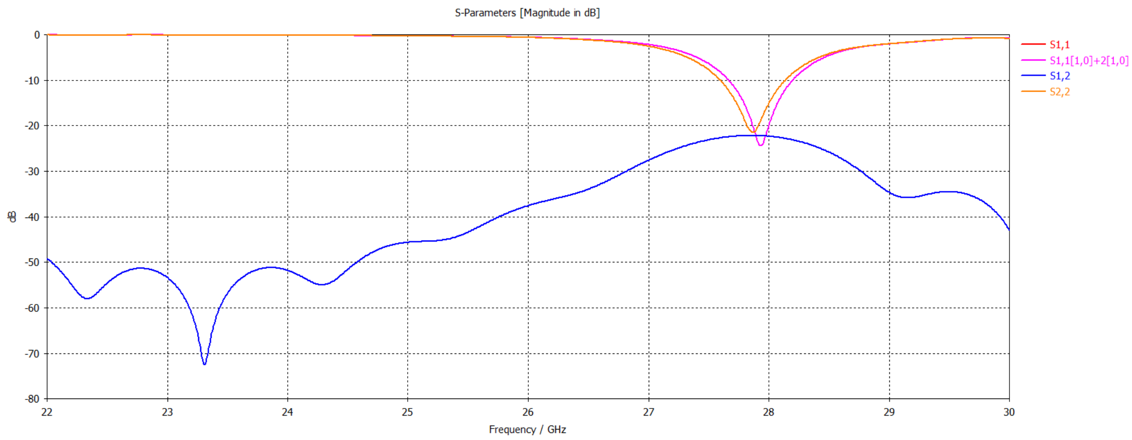

Figure 3.4: 2 by 1 patch antenna array S-parameters

3.3 Array of four patches

Next, an array with same dimensions, as in previous cases, consisting of four patches in 2x2 configuration, is simulated. The antenna separation is chosen to be $\lambda/2$ to avoid the grating lobes. In figure 3.5 combined far field pattern is plotted. Maximum gain is 11.3 dBi, 3 dB beamwidth is 51.6° Coupling in a four element array depends on the distance between the elements, being smallest for elements diagonal to each other. Gain is only slightly higher than for two element array, which could also be caused by coupling or ohmic losses, since by doubling the number of elements the gain should increase by 3 dB. The half power beamwidth is 51.8° and -10 dB bandwidth is more or less the same, as for two element array.

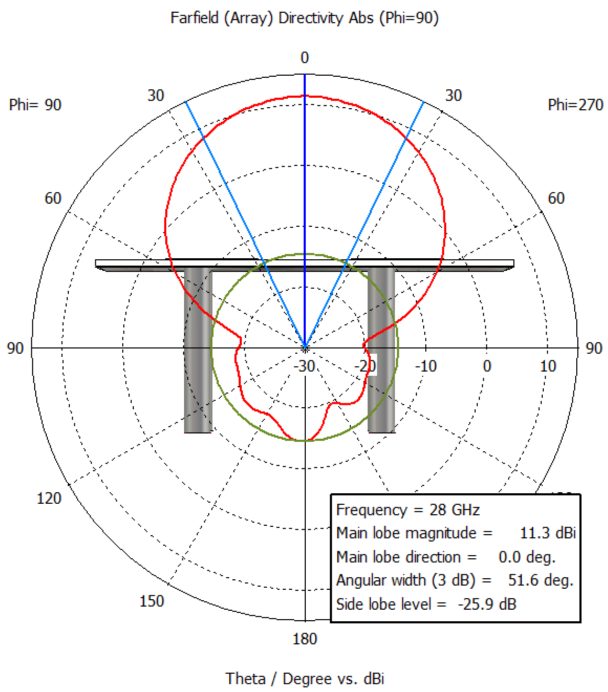

Figure 3.5: Far Field pattern of 2x2 patch antenna

Mutual coupling between the elements is plotted in figure 3.6

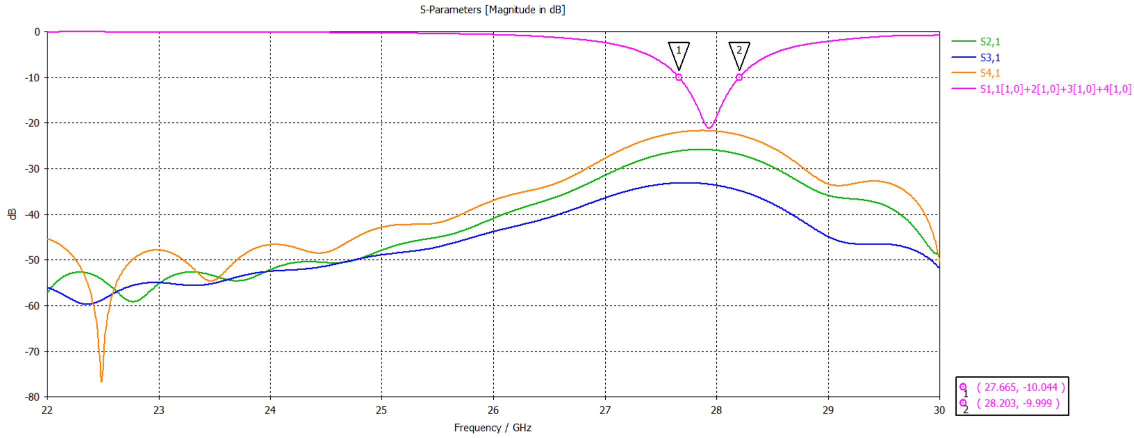

Figure 3.6: 2x2 patch antenna S parameters

3.3.1 Four by four array simulation

In order to clearly see the mutual coupling and its effects in an array a four by four array, consisting of 16 patches is made. The equispaced elements have the same dimensions as the single patch and the feeding is realized with 50 Ω coaxial cable. Center frequency was kept at 28 GHz. The structure of the array in figure 3.7. For the sake of the simulation speed the largest separation, from center to center, which was investigated was 0.4λ. At this separation distance the bandwidth is about the same, as for smaller arrays discussed earlier. This is because the separation still is large enough so that the coupling does not deteriorate the array performance significantly.

The separation between the elements is reduced in several steps and S_{11} of the array is observed. Elements are equispaced in square array and distance between the elements is reduced to illustrate the deterioration in performance caused by the coupling. The coupling has strong effects on the resonance frequency and bandwidth, when decreasing the separation between the patches the performance changes significantly, although having a slight improvement in -10 dB bandwith at 0.3λ compared to 0.4λ separation. For 0.27λ the bandwidth at -5 dB level is slightly wider than for larger separations. This could mean that the coupling has some positive effects in terms of bandwidth. By optimizing the array, it might be possible to increase the resonance and reach -10 dB level. S11 for various separations is plotted in figure 3.8.

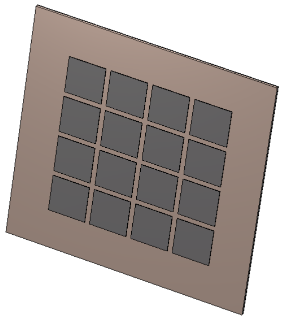

Figure 3.7: 4x4 array structure

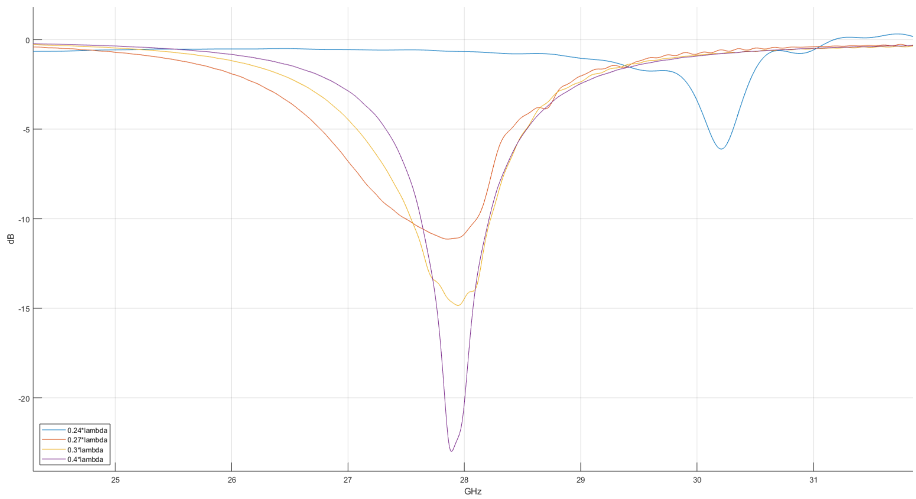

Figure 3.8: S_{11} for various patch separations

From S_{11} plot the bandwidth at most is about 2.4% at -10 dB level, this is not considered as a wide band array. In this array configuration the cause of the narrow bandwidth is most probably the feeding structure, which is realized with coaxial cables. Typical bandwidth for coaxial fed patch antenna is around 2-3% because the dimensions of the cable are dependent on the frequency and large deviations from center frequency means that the cable will not be impedance matched to the patch and therefore high reflections arise when moving away from designed resonance frequency.

3.4 Microstrip antenna feeding methods

There are many different approaches to how to feed the planar microstrip. Depending on the physical requirements and field of application the suitable feeding can be chosen. In most of the cases the bandwidth requirement is the critical factor in choosing the feeding. Some of the most common feeding methods are presented in this section together with comparisons between them.

3.4.1 Microstrip feeding

Possibly the most common and the easiest way, in terms of manufacturing, is the microstrip feed. This is probably most common as well in commercial applications, because it is realized on PCB with same metal layer as the antenna patch itself. The microstrip line is simply connected to the edge of the patch. In patch antennas the impedance is very high at the edge of the antenna and thus matching with microstrip line can be challenging. To improve the matching the feed point can moved closer to the center of the patch by making a recessed microstrip feed. In that way instead of having an input impedance around 150 to 300 Ω [19] the impedance point of 50Ω can be found. Often the exact feeding point is determined with simulations and is somewhere in between center and the edge *i.e.* between zero ohms in the middle and several hundred at the edge. However, the main disadvantage of microstrip feed is relatively narrow bandwidth, about 2-5% [19].

3.4.1.1 Probe feeding

Another common way of feeding the microstrip antenna is to use probe feeding. This is advantageous when the feeding network cannot or does not have to be on the same plane as the antenna, because of dimension limitations. Probe feed connects feeding network to the antenna underneath with coaxial cable. Similarly, as with the microstrip feed, the feeding point must be fine-tuned with simulations to achieve a good impedance matching. As presented previously the coaxial probe feed is also very narrowband $\sim 2\%$. Microstrip and probe feed both support higher order modes, which increase the cross-polarization level.

3.4.1.2 Aperture coupling

To increase the bandwidth aperture, coupled feed can be used instead [30]. With some tweaking and proper design, it is possible to design a patch antenna with bandwidth of 8%. First aperture coupled patch antenna was proposed by D. M. Pozar [31] where he used circular slot in the ground plane to excite the slot with microstrip feed line. Nowadays most of the slot coupled antennas use rectangular slots. Although achieving higher bandwidth compared to probe coupled antennas, the disadvantage of slot coupling is the dimensions of slot and matching stub, which with its $\lambda/4$ length is too long for arrays where the elements are close together as in connected arrays. The $\lambda/4$ stub can be longer than the patch itself and therefore will affect the performance of other antenna elements. Aperture coupled antennas are difficult to manufacture because of several conducting layers and precisely positioned slots.

A simple drawing of microstrip patch feeds is shown in figure 3.9. From left, the first drawing shows the "classical" microstrip feed, where the line is connected directly to the edge of the patch. Second one is the recessed microstrip weed, where there is a cutout in the patch to move the feeding point closer to 50 Ω impedance point. Thirdly a slot feed is illustrated, where the horizontal rectangle represents the slot in the ground plane underneath the patch and white dashed rectangle is the microstrip feeding line on the bottom metal layer. On the right a coaxial cable feed is illustrated, the cable connects underneath the patch.

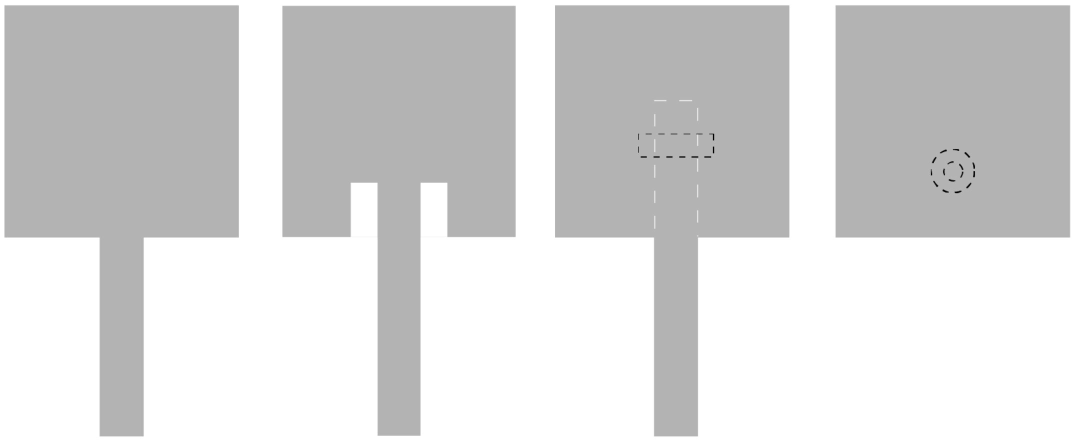

Figure 3.9: Common microstrip patch feeding methods, not to scale

3.4.2 Conclusion about the patch antenna

This chapter illustrated that a simple microstrip patch is relatively easy to design and the performance at the design frequency is fine. But it is not easy to use the patches for a high frequency connected array, which should have a wide bandwidth. This is because the feeding methods provide narrow band impedance matching. For wider band feeding, the slot, dimensions for the slot and matching stubs are too large for closely positioned antenna element geometry. From the simulations it is clear that the array performance depends on the element separation, but also the total amount of elements, parameters like gain HPBW and bandwidth were different depending on the array size.

Therefore, another solution on wide band and wide scan antenna array is investigated in the next chapter.

4

Design of the unit cell

It was shown in previous chapter that patch antennas are good for their planar structure but feeding them is a challenge. Simulated coaxial feed is quite narrowband and slot feed is difficult to manufacture and implement since slot size and matching stub dimensions are bigger than separation between two patches. Therefore, an array which consists of planar dipole antennas is investigated. As mentioned in section 1.6 there have been studies about wide band connected arrays which however are at lower frequency. Therefore, these works are taken as a reference to design a connected wide band antenna array for millimeter wave band.

4.1 Single planar dipole

A simple planar $\lambda/2$ microstrip dipole antenna is designed in CST. The dipole is made of PEC and surrounding material is vacuum. The design frequency of 8 GHz was chosen to compare the results with [3]. This frequency makes the dipole length to *ca*. 18.7 mm. Exact dimensions in terms of length, separation (gap) between the arms and the width of the dipole arms were found out through optimization. The dipole arms are fed in the center by a discrete 71 Ω port. From the antenna theory impedance of the dipole antenna at the feed point is around 73 Ω [32]. Geometry of the dipole is in figure 4.1. The width of the dipole arm corresponds to $\lambda/7$ in terms of electrical length.

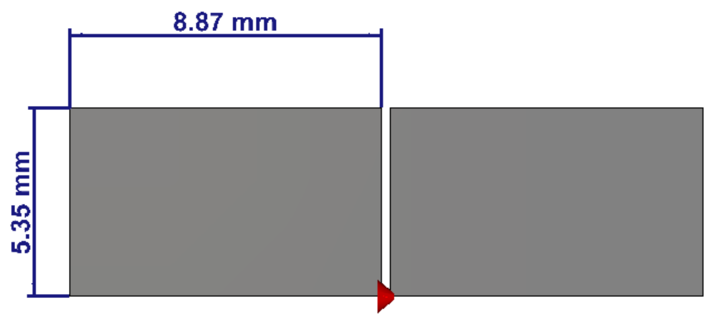

Figure 4.1: Planar dipole with discrete port feed in the center.

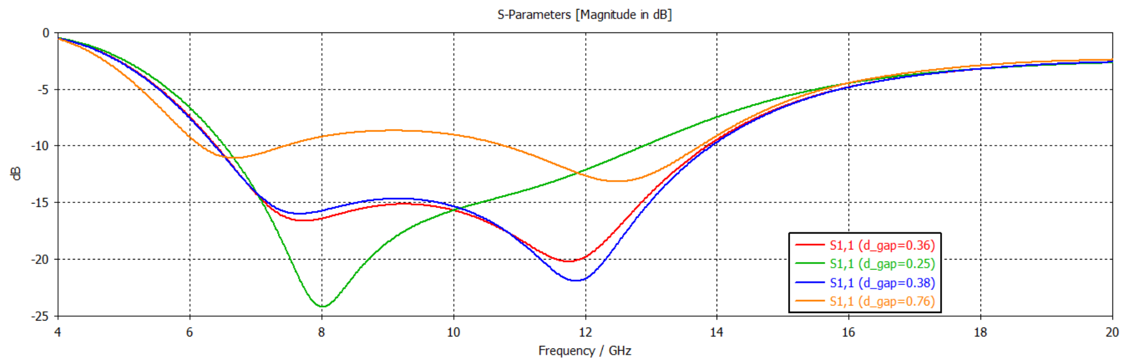

Figure 4.2: S_{11} of the planar dipole with various gap sizes.

The bandwidth of the dipole is further optimized by changing the separation between the two arms. This is seen in the S_{11} sweep in figure 4.2. Strongest resonance at 8 GHz occurs with the separation of 0.25 mm, but the bandwidth is noticeably larger with larger separation and when the separation becomes too big like with 0.76 mm the performance drops significantly.

With verified input impedance of 71 Ω for the antenna 71 Ω microstrip feeding lines were calculated. Since the "standard" formulas for microstrip lines require ground plane but here the feeding is realized with differential lines, without ground. The microstrip line from microstrip line formulas [33] was taken as a basis for the differential line design. Final dimensions were fine-tuned experimentally in CST.

The transmission lines with length of $\lambda/2$ are used because transmission line of this length does not transform the impedance and thus ideally the input impedance at the transmission lines should be the same as input impedance directly at dipole arms. Geometry of the dipole with feeding lines is illustrated in figure 4.3.

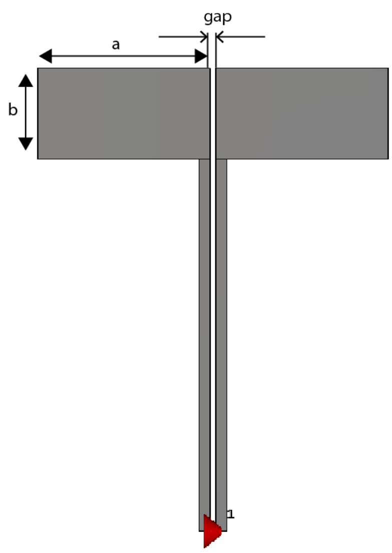

Figure 4.3: Geometry of the dipole together with feeding

For optimal performance the length of the arms, dimension a, is kept the same as in figure 4.1 and width b is slightly shortened to 4.68 mm. S_{11} parametric study is made for same gap separations as shown before in figure 4.2. Width of the feeding lines is 0.6 mm. Highest bandwidth is achieved with gap separation of 0.25 mm but when comparing the bandwidth with and without feeding lines it is apparent that the microstrip feeding lines deteriorate the bandwidth because of the bandwidth limitation of the microstrip line.

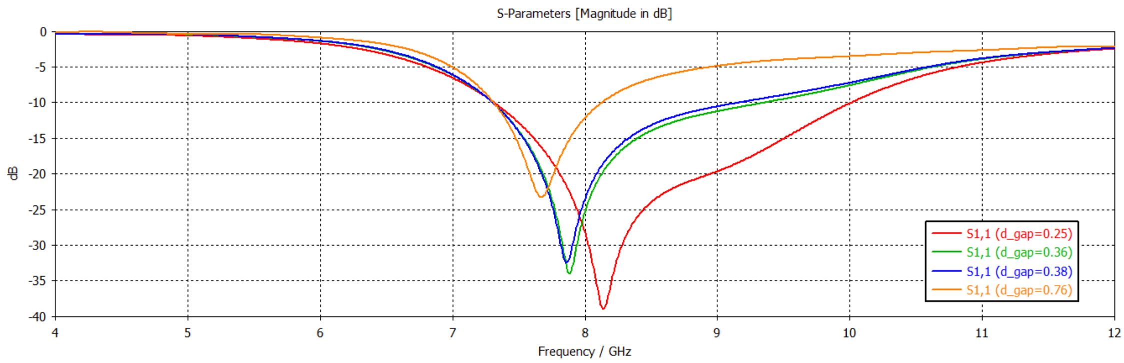

Figure 4.4: S_{11} for dipole with feed lines for different separation distances

However, it is noted that the bandwidth of the dipole is very dependent on the length of the b. When reducing the dipole arm width by two (to 2.34 mm) the bandwidth increases bit more than 1 GHz. In other words, -10 dB bandwidth is increased from *ca*. 32% to 43%. The S_{11} for gap size of 0.25 mm and b sizes of 4.68 and 2.34 mm are shown in figure 4.5, where the red line is representing 2.34 mm arm separation and green line 4.68 mm.

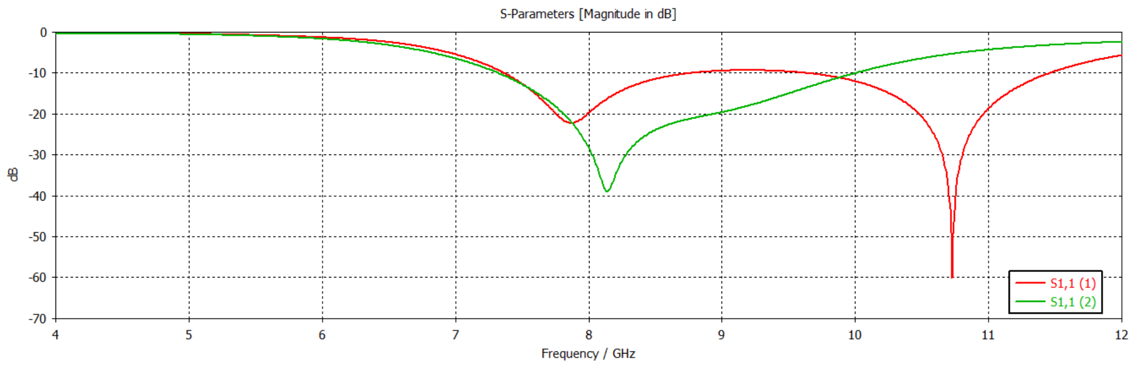

Figure 4.5: Bandwidth for dipole arm width of 4.68 and 2.34 mm in green and reed color respectively

To verify that the dipole is radiating according to the theory, a far field plot was calculated. Indeed, the radiation pattern looks like a doughnut and has maximum gain of 1.95 dBi, the theoretical gain for dipole antenna is around 2 dBi.

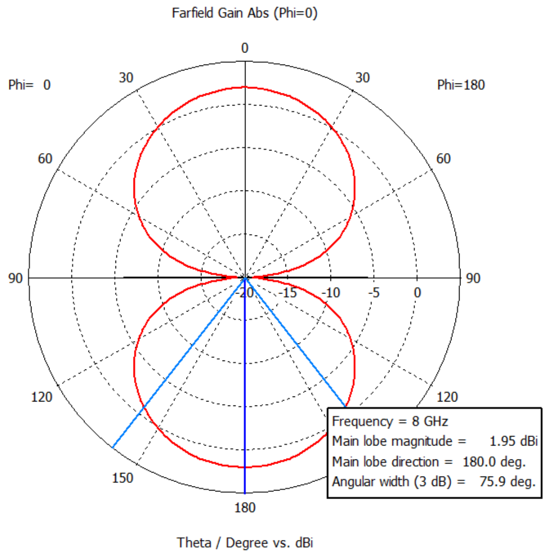

Figure 4.6: Far-field pattern of planar half-wave dipole antenna

4.2 Impedance transformer design

In dipole antennas the feeding network is a critical component in the design. As shown in previous chapter the feeding lines degrade the bandwidth of the antenna. This is because the transmission lines impedance is frequency dependent and wide band matching cannot be achieved with just transmission lines.

Commonly used impedance for power amplifiers (PA) and other components in feeding network is 50 Ω and this means that antenna 71 Ω must, for high efficiency, be matched with the impedance of feeding network. For that a simple quarter wave transmission line can be used where the length is $\lambda/4$ at design frequency and the impedance of transmission line is

$$Z = \sqrt{Z_0 Z_L}, \tag{4.1}$$

where Z_0 is source and Z_L is load impedance. However, since in the array application the active impedance of one antenna element changes depending on the scan angle the matching section must be broadband. Therefore, tapered impedance transformer is considered. One of the possibilities is to use Klopfenstein transformer. This transformer design is advantageous because it has a small reflection coefficient over passband and has a shorter matching section length compared to exponential or triangular taper [34]. Taper impedance is calculated with applet from [35] and the width of each section is calculated from impedance with (4.2)-(4.5) from [33]. MATLAB script is made which imports coordinates from the applet, calculates the widths and outputs coordinates for polygon to use as a taper in CST.

$$When \frac{W}{H} < 1$$

$$Z_0 = \frac{60}{\sqrt{\epsilon_{eff}}} ln\left(8\left(\frac{H}{W}\right) + 0.25\left(\frac{W}{H}\right)\right) \tag{4.2}$$

$$\epsilon_{eff} = \frac{\epsilon_r + 1}{2} + \frac{\epsilon_r - 1}{2}\Big[\frac{1}{\sqrt{1 + 12H/W}} + 0.04\big(1 - \Big(\frac{W}{H}\Big)^2\big)\Big] \tag{4.3}$$

$$\textit{and when} \frac{W}{H} > 1$$

$$Z_0 = \frac{120\pi}{\sqrt{\epsilon_{eff}}[\frac{W}{H} + 1.393 + 2/3ln(\frac{W}{H} + 1.444)]} \tag{4.4}$$

$$\epsilon_{eff} = \frac{\epsilon_r + 1}{2} + \Big[\frac{\epsilon_r - 1}{2\sqrt{1 + 12H/W}}\Big], \tag{4.5}$$

where W and H are width of the microstrip line and height of the dielectric respectively. However as previously mentioned the feeding lines for dipole are not regular microstrip lines but coupled microstrip lines with odd mode excitation. Because of that formulas for microstrip line calculations are different than in this application, where the feeds should act as balanced lines for dipole. Therefore a trial-and-error method is used to fine-tune the impedance of the taper in order to match antenna with 50 Ω. S-parameters for Klopfenstein impedance transformer, which transforms 50 ohms to 71 ohms are shown in figure 4.7. Left side is the low impedance input and right high impedance.

Transformer is modelled on RO4003C 1.118 mm thick dielectric with ϵ_r of 3.55. Length of the transformer is chosen so that the minima for the first ripple will be at the center frequency. This occurs approximately at $\lambda/2$ however, in the simulated design this is optimized and scaled therefore it is longer in figure 4.8.

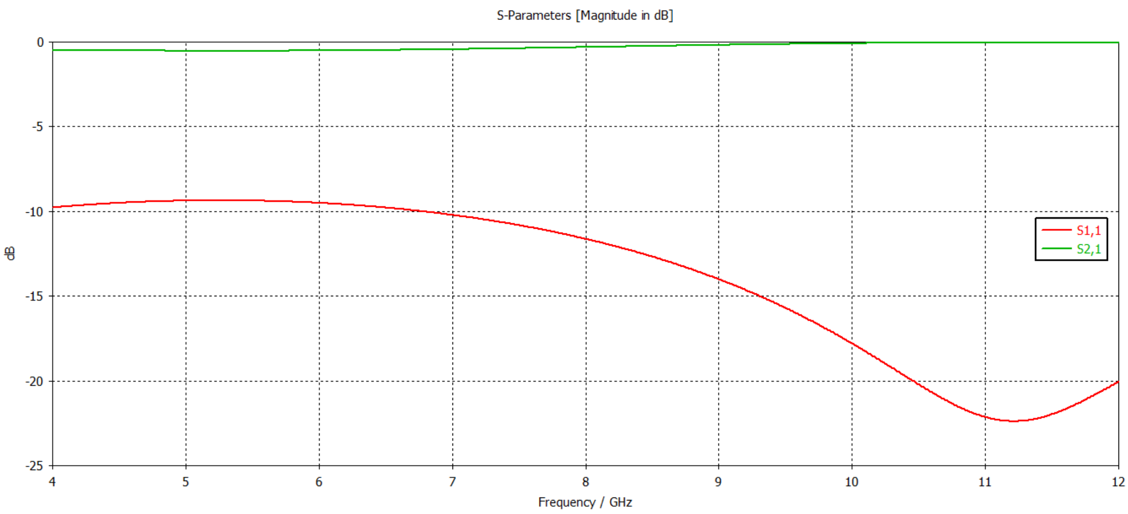

Figure 4.7: S-parameters of Klopfenstein transformer with impedance transformation from 50 Ω to 71 Ω

The return loss is not perfect although being lower than -10 dB in the frequency band of interest but S_{21} shows that the losses are very low -0.35 dB at 8 GHz, which is good. The problem however arises when looking at the dimensions of the transformers, which are very small. Even at this frequency of 8 GHz it is not possible to manufacture the transformer cheaply on the regular PCB. It is possible that with clever optimizations the dimensions which are within manufacturing capabilities can be found, but since it could be very time consuming another solution is investigated. Also, since the transformer in this configuration is very dependent on the separation between the lines it is difficult to match the impedance from transformer separation and antenna gap size.

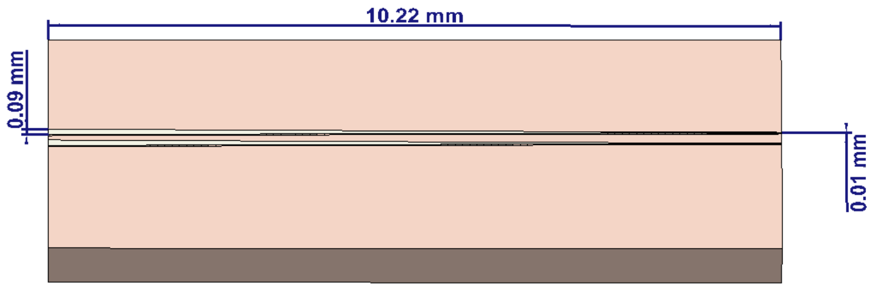

Figure 4.8: Geometry of the Klopfenstein transformer

4.3 Impedance transformation with BALUN

Instead of using a tapered transformer as differential feeding lines a tapered BALUN is considered.

4.3.1 Working principle of the BALUN

The name BALUN comes from BALanced to UNbalanced which states that BALUN changes balanced signal to unbalanced and vice versa. There are two common feed line modes, balanced and unbalanced lines. On a PCB signals in most of the cases are unbalanced, this means that the impedance of the signal trace is different compared to the impedance of the ground signal. This because circuit boards tend to have much bigger ground plane, compared to signal traces, which has lower impedance because of its large size. In many applications, like feeding networks and in planar patch antennas the unbalanced signal is fine, since large ground plane is assumed to be infinite and it is what most of the components require. It is common to feed the antennas with coaxial cable, which is unbalanced. This is fine for example monopole and patch antennas, which have a large ground plane. However, for certain applications, like dipole antenna the feeding signal should be balanced and differential feeding should be used.

In dipole antennas, when feeding with coaxial cable, the inner conductor is connected directly to one dipole arm, but outer conductor is connected to other arm so that part of the current from inner conductor flows in outside part of the outer conductor back to the ground. With BALUNs current flow outside of the outer conductor to ground can be blocked by making the impedance between outside conductor to ground infinite.

Another option is to cancel out the currents with opposite phases. This can for example be realized by connecting $\lambda/4$ transmission line so that one end is connected to the outer conductor of the feed and another to the dipole arm where inner conductor of the feed line is connected. Since wavelength is frequency dependent it is a challenge to make a good performance wideband BALUN and thus a wideband antenna.

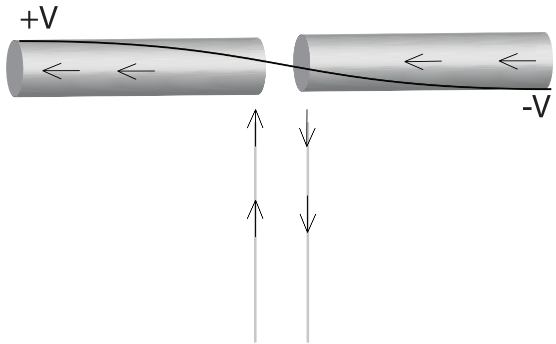

Figure 4.9: Voltage distribution of a dipole antenna

4.3.2 Common and differential modes in feed lines

Balanced transmission lines, which are used for example dipole antenna feeding, support both common- and differential modes. Differential mode is also called as normal mode [36] is the mode when signals in transmission line pair flow in opposite direction. When signals flow at same direction the mode is called common mode. In dipole antenna feeding signal should be differential, however the feeding lines are easily excited with common mode signals for example when steering the beam. Common mode signals may create unwanted noise or radiation from the feeding lines. To suppress the common mode a choke can be used. In design-wise easiest common mode choke is a ferrite core around which the transmission lines are winded in a way that magnetic fields are in opposite direction and cancel out suppressing the common mode. Ferrite core choke has few drawbacks, first it works on low frequencies only [3] and secondly it is hard to fabricate and implement on a single planar structure.

Centre fed dipole antenna has equal voltage magnitude but 180° phase difference. This yields maximum radiation efficiency, reduces noise, by rejecting the common mode and ensures that the feed line does not act as radiator. Voltage distribution of a dipole is in figure 4.9.

4.3.3 Planar BALUN

Certain applications require that the BALUN is planar and printable on the circuit board for ease of manufacturing. In this phased array antenna, it would be convenient to implement the BALUN on the same structure as the antenna elements. Some of the planar BALUN designs are discussed in [37] where most of the designs compared achieve a bandwidth of ca. 7-8 GHz at design frequency around 5 GHz. One design, where microstrip to slotline transition BALUN is designed has bandwidth from 4 to 45 GHz. In this work a planar tapered BALUN is investigated.

4.3.4 Tapered BALUN

Tapered BALUN is quite similar to the Klopfenstein impedance transformer where the lower impedance is gradually transformed to higher impedance with a tapered microstrip line. At the same time in tapered BALUN the signal is converted from unbalanced signal to balanced. A BALUN to transform 50 Ω to 71 Ω is designed. It is shown in figure 4.10. The BALUN consists of three-layer PCB- top metal layer, noted with red rectangle; dielectric in blue and bottom metal layer as a taper. For verifying that the input signal is unbalanced a coaxial feed is connected to the BALUN with inner conductor touching top metal and outer conductor bottom metal.

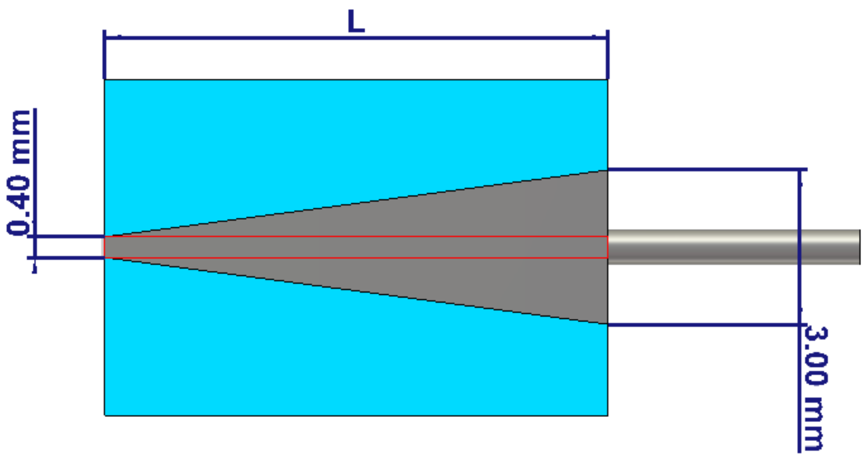

Figure 4.10: Tapered balun from 50 Ω to 71 Ω

This designed BALUN has good performance over a wide bandwidth and the dimensions are suitable for regular PCB manufacturing. Output impedance depends on the width of the top metal line, which is constant over whole BALUN length, while the tapered line transforms the impedance to same level as the top conductor. The length L of the transformer is changed, and S-parameters are observed. Theoretically with longer transformer the bandwidth is higher since the impedance is transformed more smoothly.

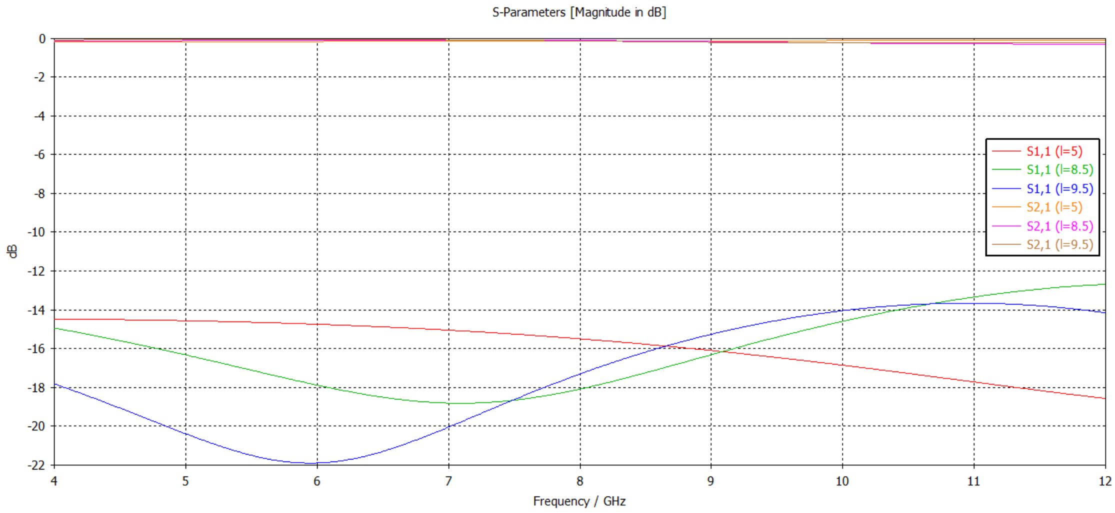

Figure 4.11: Tapered BALUN S-parameters with different taper lengths.

The downside which is discovered with this BALUN is the performance dependence of the output impedance. In scanning array, the impedance changes depending on the scanning angle and therefore the BALUN should also have good performance when the impedance differs from design impedance. With this BALUN the return loss increases by at least 4 dB when the impedance is 91 Ω instead of the designed 71 Ω.

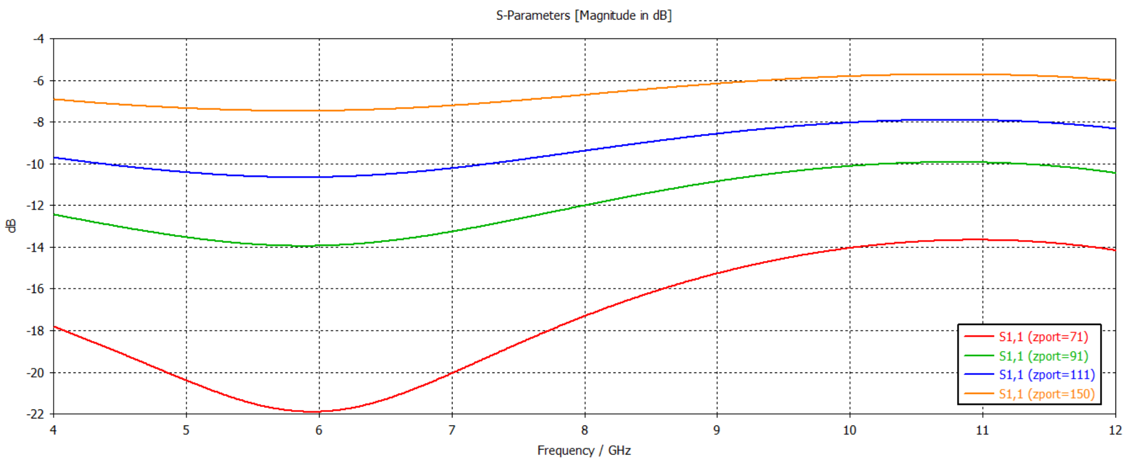

Figure 4.12: Return loss for tapered BALUN when sweeping impedance

Apart from small tolerances in output impedance this BALUN shows promising results and might be considered in an application where the output impedance is not altering.

4.4 Loop shaped transformer

For the reasons described in previous sections a different solution is investigated. Two solutions are presented in [3] where one possibility is to make the feeding lines shorter, so that the common mode resonance is shifted from the antenna resonance frequency. However, the disadvantage with this solution is that the bandwidth of choke is dependent on the load (antenna) input impedance, so wide a bandwidth is achieved when the antenna input impedance is low.

The second solution is to use a loop shaped transformer. This works similarly as ferrite core choke, where at higher frequencies currents along the loop have different phases and therefore create magnetic fields which are in opposite directions and cancel out the common mode currents. The loop solution also provides impedance transformation which is advantageous since then impedance transformation from 50 Ω to antenna impedance can be matched in several steps over a longer physical length. Longer matching section provides larger bandwidth. The structure of the loop shaped common mode choke is in figure 4.13.

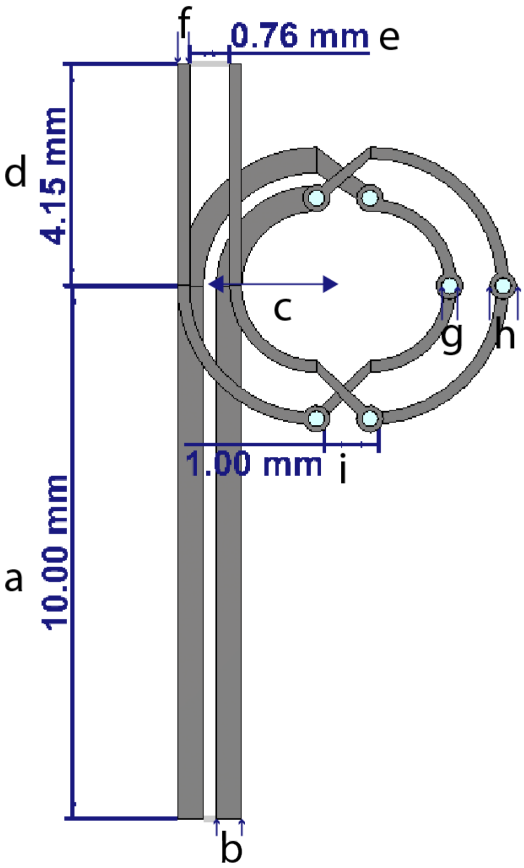

Figure 4.13: Geometry of the loop shaped common mode choke

For verifying the performance of the loop, which is presented in [3], the transformer is simulated with exactly the same dimensions. Not shown in the figure are the widths of the microstrip lines, where at the bottom the width is 0.48 mm and at the output on top 0.22 mm. The structure consists of three layers- top and bottom metal and dielectric in between. VIAs are used to connect the two layers and since the inner loop radius is smaller than outer the VIAs are also needed to "shift" the loop radius to make both transmission lines equally long. Total length of the loop is $\lambda/2$. The input impedance at the bottom of the loop is 100 Ω and at the output 350 Ω.

Return loss is plotted in figure 4.14 and compared against the reference values. Frequency domain result is not the same, but comparable to the one in [3]. Two different output impedances are used because when 350 Ω (green in fig. 4.14) is active, the impedance the loop "sees" the antenna to be according to calculations in [3] but as shown in the graphs the performance increases when having an output impedance of 200 Ω. The resonance seen in the figures around 3 GHz is most probably caused by the shape of the transformer. The loop acts like a ring resonator where the dimensions of the loop are favorable to have a strong resonance at 3 GHz. In the reference there is not enough information how the resonance is cancelled, but probably the lines to VIAs are tweaked.

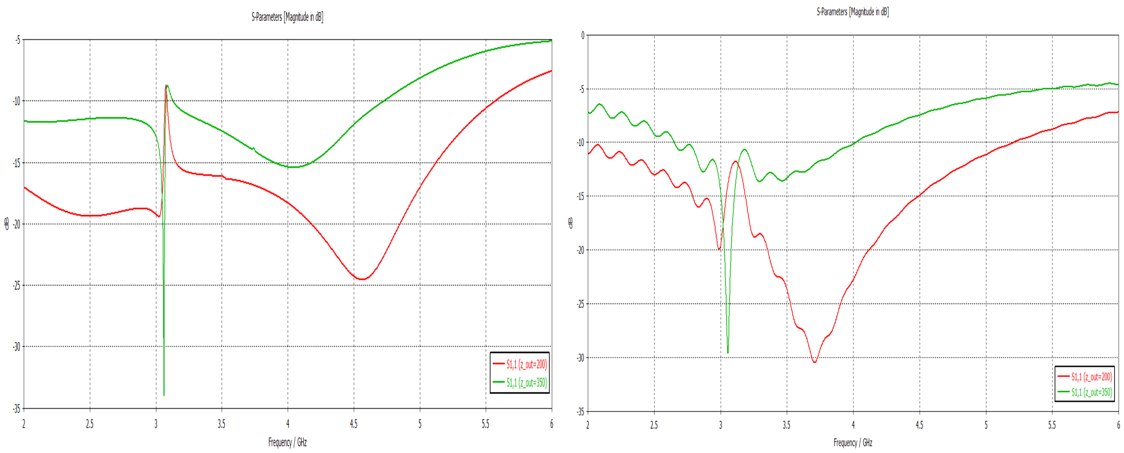

Figure 4.14: Loop transformer return loss frequency- (left) and time domain (right)

4.4.1 High frequency loop transformer

After verifying that the loop performance is satisfactory the loop dimensions are scaled in frequency for the operation in 23 GHz and up. Scaled dimensions of the loop are in the table.

Parameter	Dimension	Size at f_c 4 GHz [mm]	Size in λ	Size at 23 GHz [mm]
a	Input feed length	10	0.133	1.738
b	Input feed width	0.48	0.006	0.083
c	Loop radius	2	0.026	0.348
d	Output feed length	4.15	0.055	0.721
e	Output feed separation	0.76	0.010	0.132
f	Output feed width	0.22	0.003	0.038
g	VIA inner diameter	0.3	0.004	0.052
h	VIA outer diameter	0.5	0.006	0.086
i	VIA separation	1	0.013	0.173

Table 4.1: Dimensions of the loop shaped transformer

As it might be seen directly form the table 4.1 the dimensions at 23 GHz are very small and are outside of the standard commercial PCB manufacturing capabilities. One of the smallest dimensions is the output feed width, which by scaling should be 0.038 mm. However, checking the manufacturing capabilities from for example [38], [39] the minimum allowed trace width is 0.1 mm. Another parameter is VIA diameter, which by scaling should be 0.052 mm, but the minimum allowed is 0.15 to 0.1 mm. Therefore, the loop was basically redesigned from the beginning by having the minimum manufacturing limitations as guidelines. Trace separation, VIA hole size and trace width were the key parameters which were followed when designing the loop.

It was observed that the performance very much depends on the VIA separation, input and output line length and the separation between the lines. Multiple sweeps with various parameter combinations were made to make the loop functional at higher frequency.

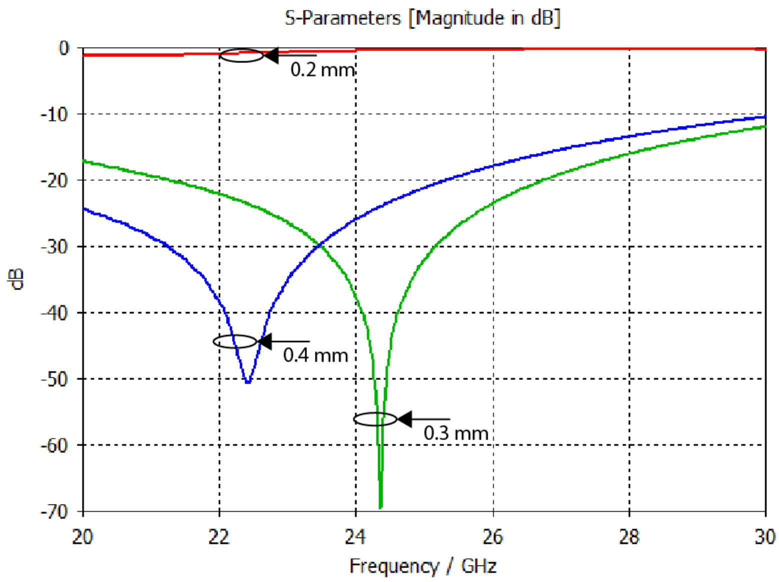

Figure 4.15: Sweep of VIA separation

In figure 4.15 VIA separation is swept for three values 0.1 mm different from another. The separation shown in the figure is the distance from center to center, so for distance between VIAs, or clearance in PCB manufacturing terms, 0.2 mm should be subtracted since this is the VIA radius. At the closest distance between VIAs, the VIAs touch each other and return loss is very high. With larger separation return loss changes significantly. Return loss is smaller when the separation is small and with the VIA separation the operating frequency can be tuned. During the optimization it was observed that lower separation yields better bandwidth and lower S_{11} values.

Using the best VIA separation, 0.3 mm, the length of the input feeding lines is swept. The dependence of the input feeding line length for the whole loop is similar as with other parameters. Small changes in dimensions shift the operating frequency. 1.9

mm is taken as the length of the lines for the loop. This is because it has the lowest reflection coefficient and largest bandwidth.

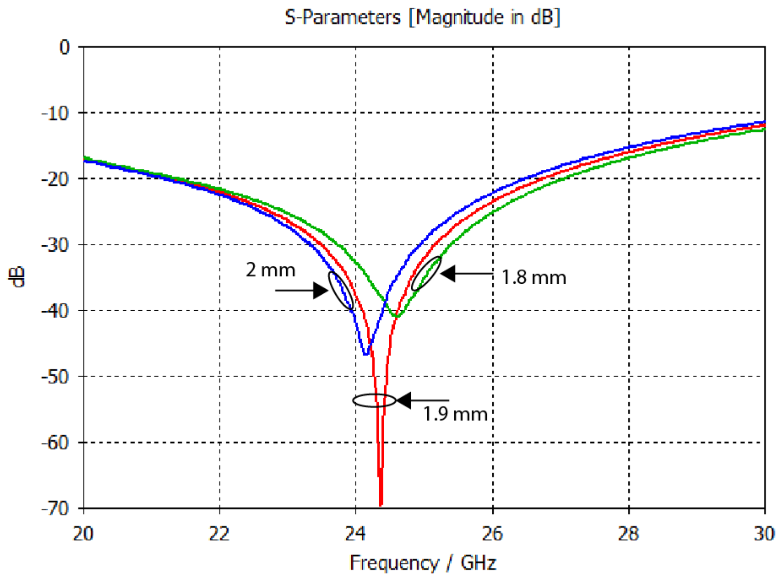

Figure 4.16: Sweep of the input feeding line length

The third major contributor to the performance of the loop, output microstrip length, is also swept. It is the length of the output microstrip lines after the loop. For this sweep VIA separation is kept at 0.3 mm and length of the input feeding lines is 1.9 mm.

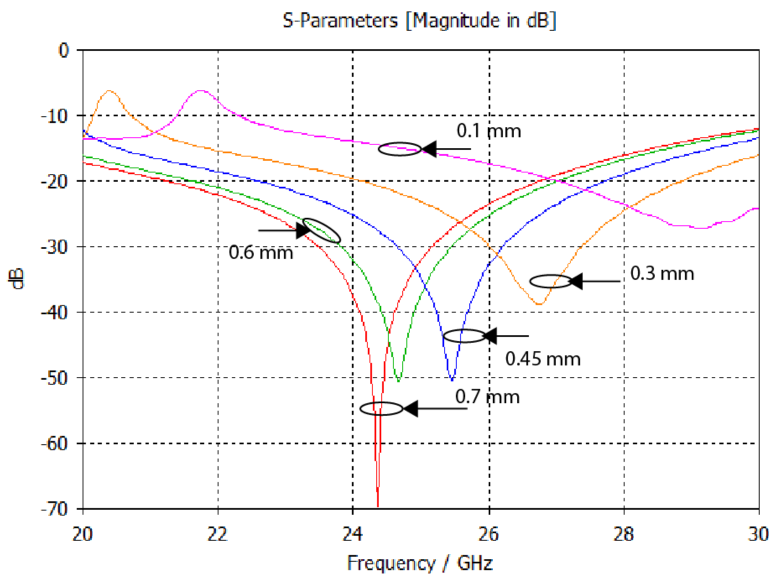

Figure 4.17: Sweep of the output feeding line length

Good return loss is achieved when feeding lines at the output have lengths of 0.7 mm. With this length the overall lowest reflection is achieved. From figure 4.17

the return loss seems to be below -10 dB for whole simulation window therefore, the simulation window is increased and the performance at higher frequency is observed. It was found that at 34 GHz the return loss is over -10 dB, illustrated in figure 4.18. Therefore, the same dimensions would not work for higher frequencies.

The dielectric constant is also increased to observe the changes. It is seen that the return loss depends much on the relative permittivity. So far used ϵ_r of 2 gives good results but might not be optimal in price and manufacturing terms. ϵ_r of 3.55 was used as a comparison, but the results were nor satisfactory so for now the dielectric constant of 2 is used.

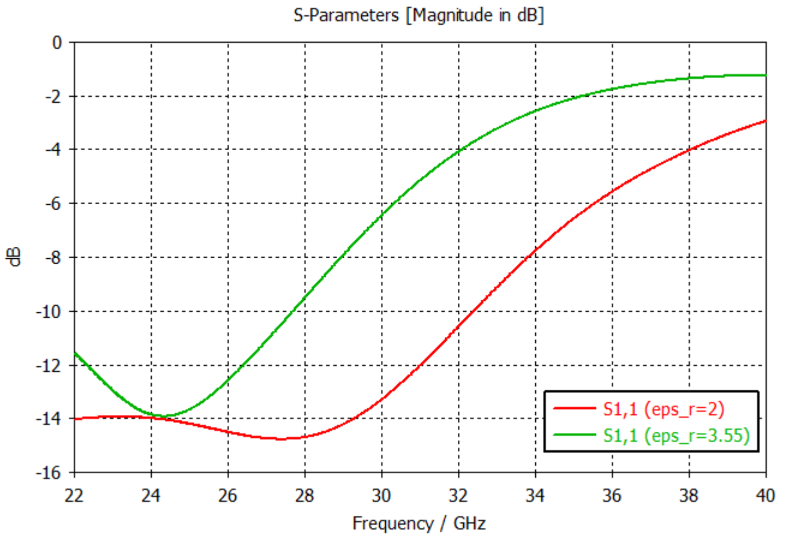

Figure 4.18: Return loss when changing the dielectric constant

The loop is tweaked to so that the dimensions are within the manufacturing capabilities of PCB. After optimizing the loop following dimensions were used:

Parameter	Description	Size at 23 GHz [mm]	Optimized size [mm]
a	Input feed length	1.738	1.9
b	Input feed width	0.083	0.12
c	Output feed length	0.721	0.7
d	Output feed separation	0.132	0.23
e	Output feed width	0.038	0.1
f	VIA inner diameter	0.052	0.15
g	VIA outer diameter	0.086	0.2
h	VIA separation	0.173	0.1

Table 4.2: Dimensions of the optimized transformer

Used dielectric has the thickness of 0.203 mm and dielectric constant 2.

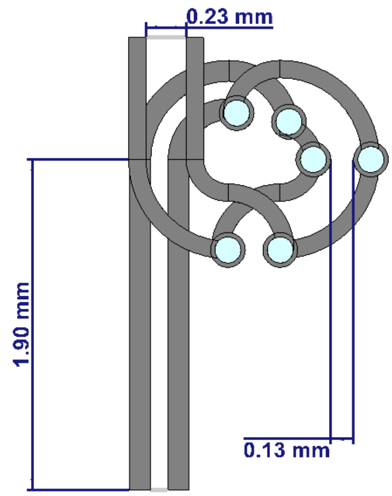

Figure 4.19: Dimensions of the optimized loop

In figure 4.19 is an illustration of the loop transformer, for clarity the dielectric layer is hidden on the figure. The dimensions are suited for PCB manufacturing capabilities and therefore there are some differences compared to the reference design. For example, the connections to the VIAs are arcs instead of straight lines, to keep the separation. It seems that the bent lines to VIAs also attenuate the strong unwanted resonance which was present on the reference model. Reflection coefficient of this transformer is in figure 4.20.

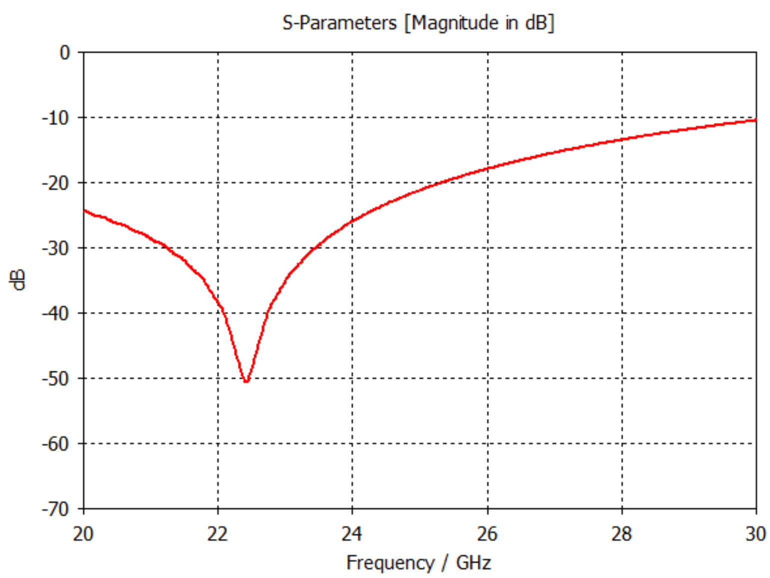

Figure 4.20: Return loss of the optimized loop transformer

4.5 Wide band dipole

After optimizing the loop, it was used as a feed for the dipole antenna. The half wave dipole has length of 8.02 mm and arm width of 0.93 mm. Structure of the dipole with loop feeding is in figure 4.21.

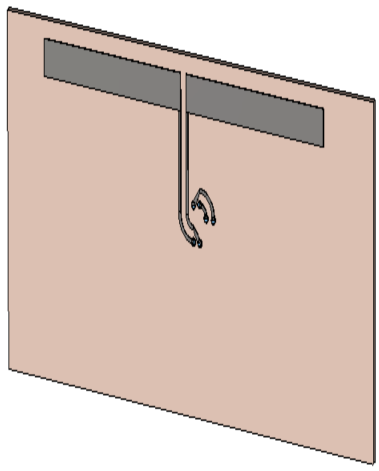

Figure 4.21: Structure of the half-wave dipole with loop feed

Radiation pattern and S_{11} are plotted in figure 4.22

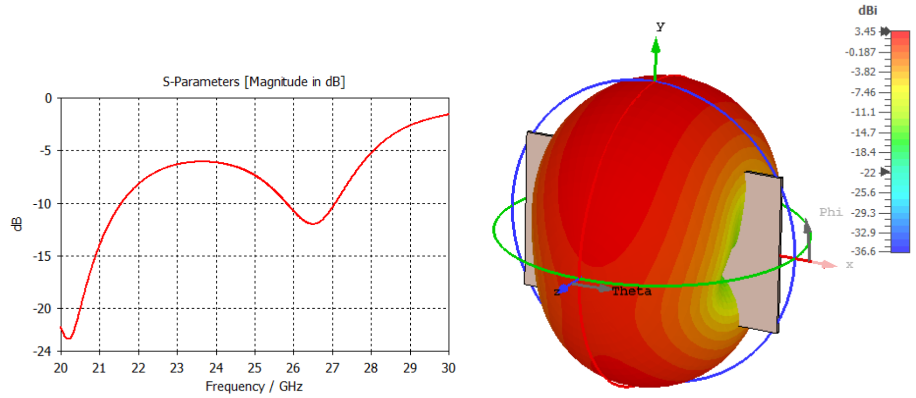

Figure 4.22: S_{11} and farfield pattern of the dipole

The dipole has characteristic radiation pattern that resembles a doughnut, although having slightly higher directivity than a simple wire dipole has. This is because the dipole is not exactly radiating as a wire dipole does, due to the the feeding structure and dielectric. The return loss is not quite in the desired frequency range being higher than -10 dB in a major part of the frequency range of interest.

For improving the antenna performance, a second dielectric layer was added on top of the core dielectric, seen in figure 4.23. This dielectric widens bandwidth and flattens the S_{11}. This effect is present because the dielectric has higher permittivity than the core dielectric and therefore slows down the radiating waves and more frequencies are coupled. The thickness of the second dielectric is 0.05 mm and ϵ_r is 2.5.

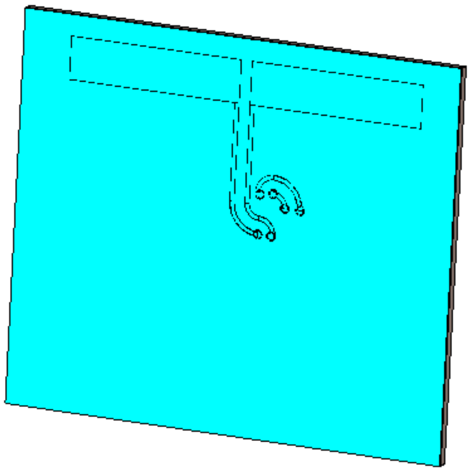

Figure 4.23: Structure of the two-dielectric half-wave dipole with loop feed

For two-layer dielectric the gain of the antenna is lower than for without dielectric, but the operating bandwidth is wider and therefore a multiple dielectric structure is considered to yield better results compared to the single dielectric.

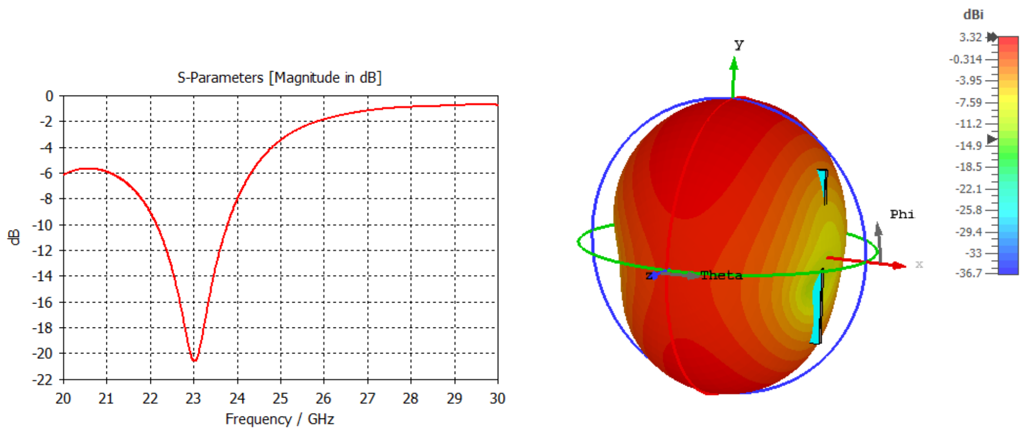

Figure 4.24: S_{11} and farfield pattern of the dipole with dual dielectric layer

The effect of the second dielectric is more clearly shown in the figures 4.25, 4.26 where the wider bandwidth, although being outside the target frequency band, is wider. The percentage bandwidth is about 10% larger, than for the configuration without second dielectric layer. In the figures the input impedance is swept to find the optimal value for antenna feeding. As mentioned previously the low S_{11} band is lower than the desired frequency range, but at this point the important note is that by adding an additional dielectric layer the performance of the antenna can be increased although a frequency shift occurs.

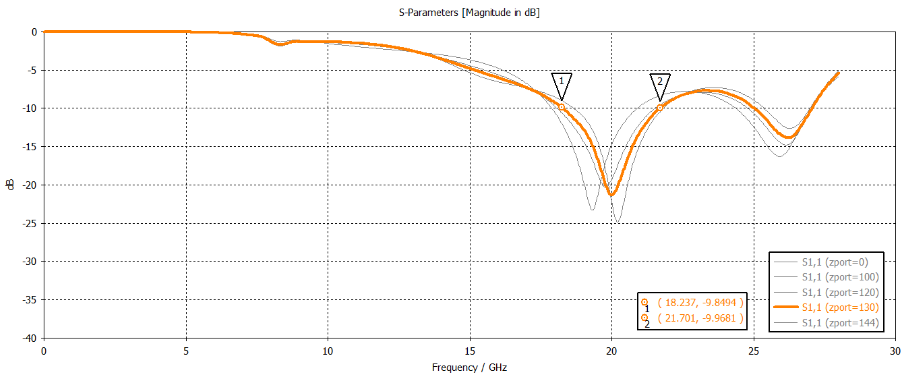

Figure 4.25: S_{11} over wide band for dipole with one dielectric

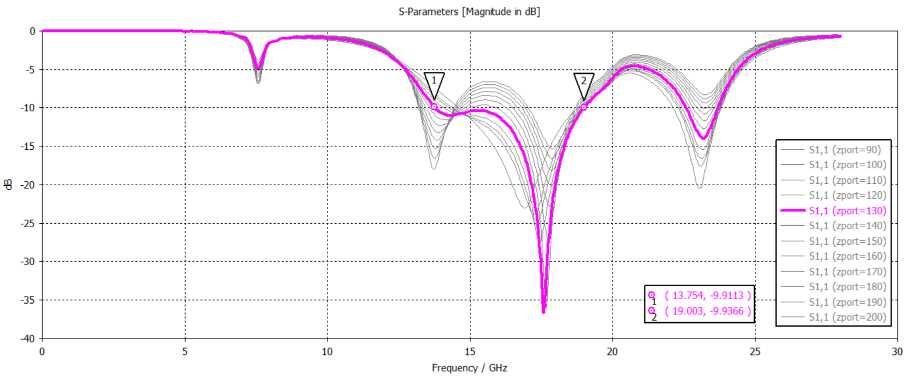

Figure 4.26: S_{11} over wide band for dipole with two dielectrics

Many different superstrate configurations were investigated and simulated to improve the bandwidth of the unit cell. Some of the geometries are in figure 4.27.

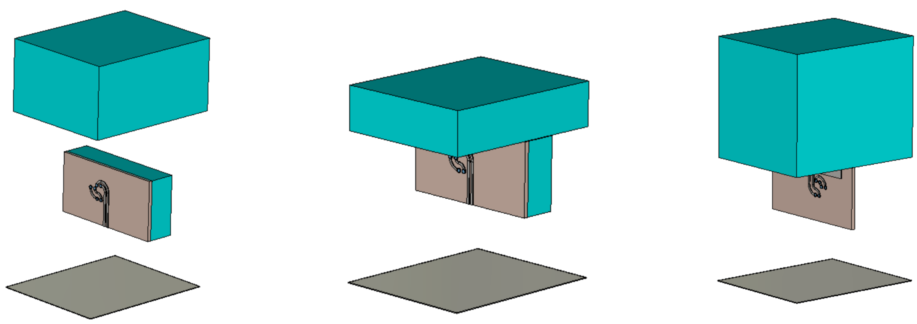

Figure 4.27: Different dielectric configurations for unit cell

In the configurations shown in figure 4.27 the ground plane is added to direct the radiation from the dipole only upwards. Thickness, relative permittivity of the dielectric layers and ground separation are swept to optimize the bandwidth of the antenna.

Initial configuration with the dielectric covering whole antenna and feeding structure was found out to give best results in terms of bandwidth.

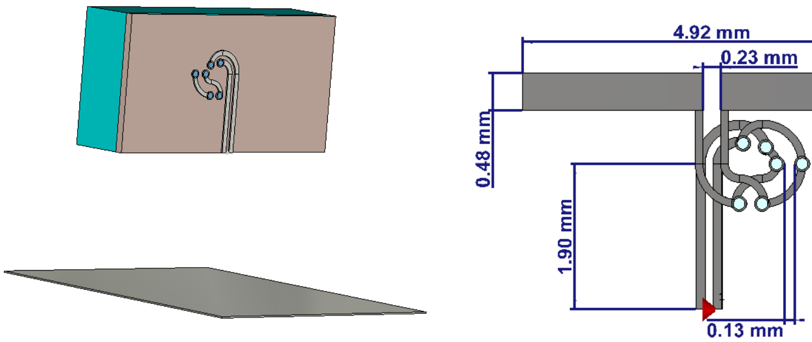

Figure 4.28: Geometry of the wide band dipole

In figure 4.28, colored in blue is the superstrate on metal layer with thickness h=1.45 mm with ϵ_r=4, thickness of the dielectric is $h_{dielectric}$=0.203 mm with ϵ_r=2, ground plane separation 3.35 mm from the bottom of the loop structure, VIA hole size is 0.15 mm and impedance at the input of the loop is 200 Ω.

This optimized dipole, with loop feeding has a wide bandwidth from 23 to more than 30 GHz GHz at -10 dB level. First mode resonates around 23 GHz, while other strong resonances which are visible on the S_{11} plot are higher order modes. Higher order modes do not have the same radiation pattern shape as the dipole by default has, but the gain in whole frequency range is from 5 dBi to more than 7dBi, which is good. The radiation patterns for 24 and 27 GHz are in figure 4.30. Although having a radiation pattern, which is bit distorted the wide band performance looks promising and an attempt is made to make an array of this unit cell. First the unit cell will be simulated in the infinite array and later in finite array with correct dimensions.

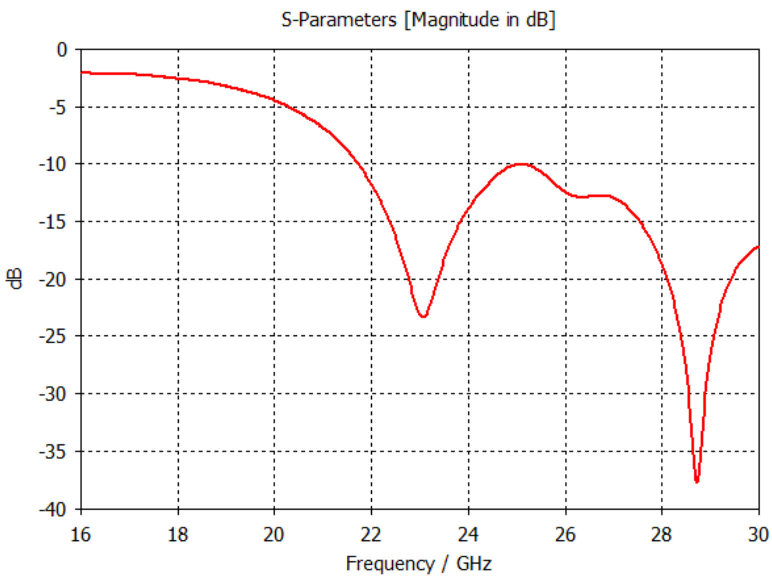

Figure 4.29: S_{11} of the wide band dipole

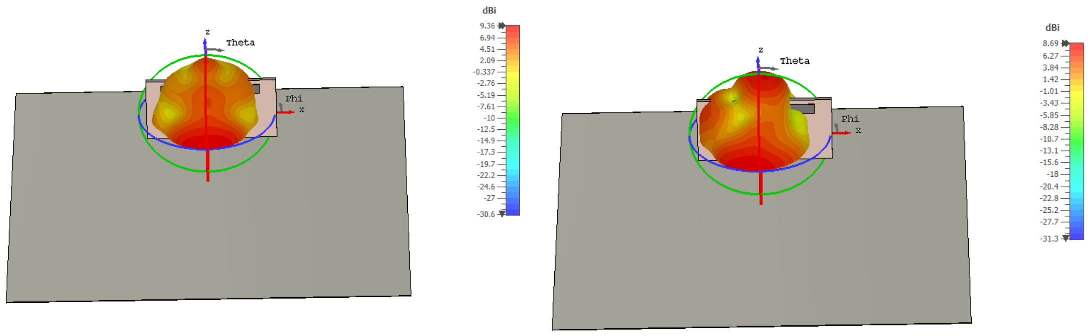

Figure 4.30: Far filed patterns for the wide band dipole, from the left 24 and 27 GHz respectively

5
Full Array

Next step in the antenna array design process is to perform the array simulation. The optimized unit cell is used as an antenna element in the array. First the required number of antennas in the array for desired gain is calculated. From eq. 2.10 the required amount of antenna elements is calculated to be 484 for the gain of 30 dBi, by taking the gain of single antenna to be 3 dBi. The unit cell, which was presented in previous section, in figure 4.28 is used as a single element in the array.

5.1 Unit cell in an infinite array

The performance of the unit cell in the array is first simulated in an infinite array. In CST by using a unit cell simulation with unit cell boundaries an infinite array simulation is carried out. Unit cell simulation in infinite array shows the radiation, surface current and S-parameters for one element as it would be in in the array in presence of other active elements. Active elements are the elements which radiate at the same time as the antenna element which is observed. Antenna separation in this simulation is $\lambda/2$ at 23 GHz in both x and y direction. S_{11} is plotted in figure 5.1.

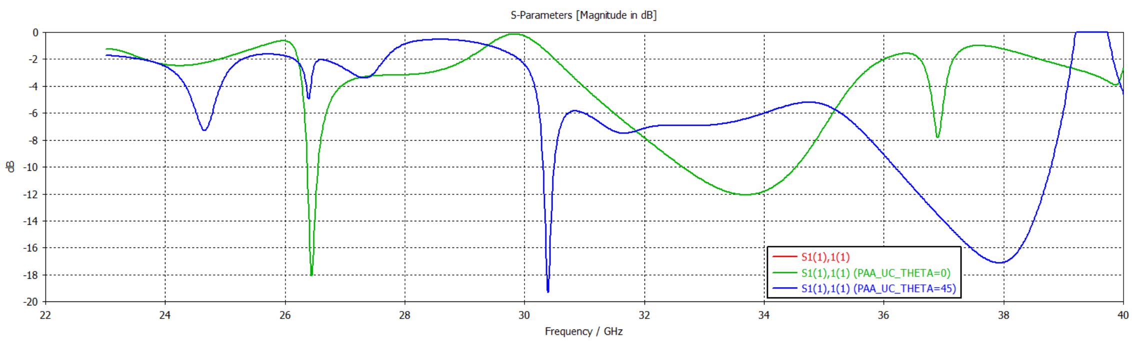

Figure 5.1: Unit cell in infinite array

In the plot green curve represents the radiation towards broadside and blue curve is elevation scan. Radiation is very inconsistent in both broadside and Theta 45° direction and the bandwidth is narrow. When scanning the impedance changes, the active impedance of the elements is higher than at broadside direction and therefore the resonance frequency is shifted up. This is seen in the figure 5.1 where resonance at broadside occurs at 34 GHz and at Theta 45 degrees around 38 GHz. From this simulation it is concluded that the initial unit cell design is not good enough and further optimization is needed.

5.2 Further optimization of the unit cell

For improving the unit cell further an attempt of using a bowtie antenna instead of standard planar dipole is made.

5.2.1 Bowtie antenna

Bowtie antenna is a broadband dipole like antenna, which, as the name states, looks like a bow tie [40]. Since the antenna size is same in terms of wavelength for each frequency ideally an infinitely long antenna has infinite bandwidth. In practice the size is almost always the limitation and therefore compromises in length vs bandwidth are made. Design equations for bow tie antenna are extracted from [41]. Side length of one arm:

$$a = \frac{2c}{2f\sqrt{\epsilon_r}} \tag{5.1}$$

and effective length of the arm

$$a_{eff} = a + \frac{h}{\sqrt{\epsilon_r}}, \tag{5.2}$$

where c is speed of light in vacuum, ϵ_r relative permittivity of the dielectric and h is height of the dielectric. Another design parameter is the angle θ which the side b is dependent on. Basic geometry of the bow tie antenna is in figure 5.2. Length b is calculated using trigonometry.

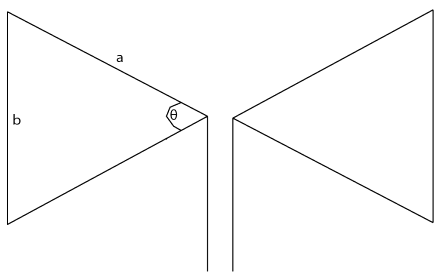

Figure 5.2: Geometry of the bow tie antenna

However, it was found that for good return loss the angle Θ must be big, close to 90 degrees and also the length a of the arm is longer than the dipole which was previously investigated and the neither was the bandwidth as wide as for dipole antenna.

5.3 Final design of the unit cell

Since the dipole was better than patch and bowtie antennas the dipole is once more looked carefully into. First a further study of changing the dielectrics is made, like the one mentioned in section 4.5. Instead of having the second dielectric covering the whole structure only dipole arms were covered, and the core dielectric was sandwiched in between the top dielectric *i.e.* superstrate. However, the biggest change was to change the dipole arm geometry, by increasing the gap distance and having a similar design as in [3]. Designed geometry of the final unit cell is in figure 5.3.

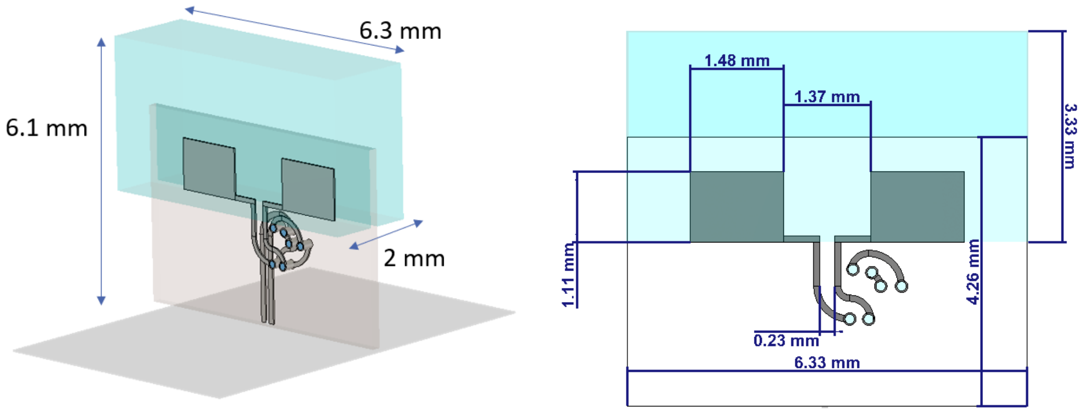

Figure 5.3: Structure of the final unit cell

The unit cell has total height of 6.1 mm, length 6.33 mm and with of 2 mm. The width considers the width of the superstrate and not the width of the ground plane, since the ground plane in final array is uniform in the array and has the length equal to the total array.

Compared to previously investigated solutions, here the gap between the dipole arms is larger than before, being 1.37 mm instead of 0.23 mm and from that the length of the arms are shorter, 1.48 mm instead of 2.35 mm. The total length of the dipole is now 4.33 mm (ca. 0.3λ) instead of 4.92 mm. The core dielectric has the dielectric constant of 2 and thickness of 0.203 mm, and top dielectric, in light blue, has ϵ_r of 5. Ground separation from the bottom of the loop is 0.1 mm. Return loss of the final unit cell design is plotted in figure 5.4. The bandwidth at -10 dB level is about 3.6 GHz with f_c of 25.5 GHz, but when relaxing the return loss criteria to -8 dB the bandwidth is around 10 GHz and actually is covering the interesting frequency band from 23 to 30 GHz. With higher return loss the gain might not be as high as wanted, but since the unit cell will be in the array this can be compensated.

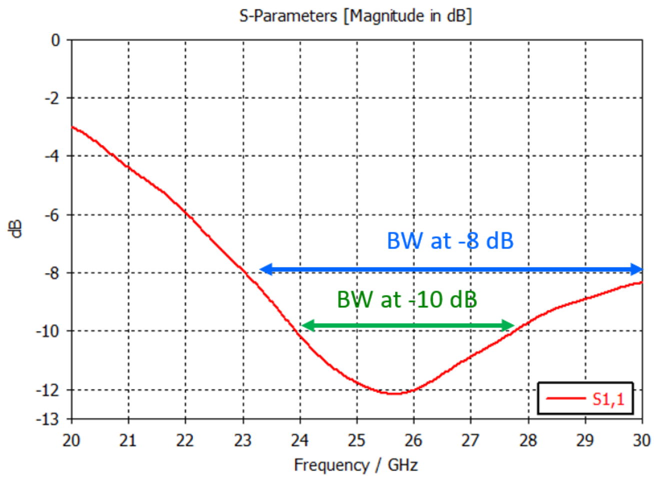

Figure 5.4: S_{11} of the final design of isolated unit cell

This unit cell design yields nice upwards-directed radiation pattern with gain of 6.6 dBi. Compared to theoretical dipole antenna gain of 2 dBi the gain is higher because of the ground plane, which directs the radiation only upwards and by that additional 3 dB is gained. Also, the top dielectric slows the wave down and therefore the radiation is directed more to the broadside, since the dielectric to broadside is thinnest. Compared to previous design the side lobe level is much lower, sidelobes in this design are about 14 dB lower than the main lobe. Polar and 3D farfield patterns of the final unit cell design are shown in figure 5.5.

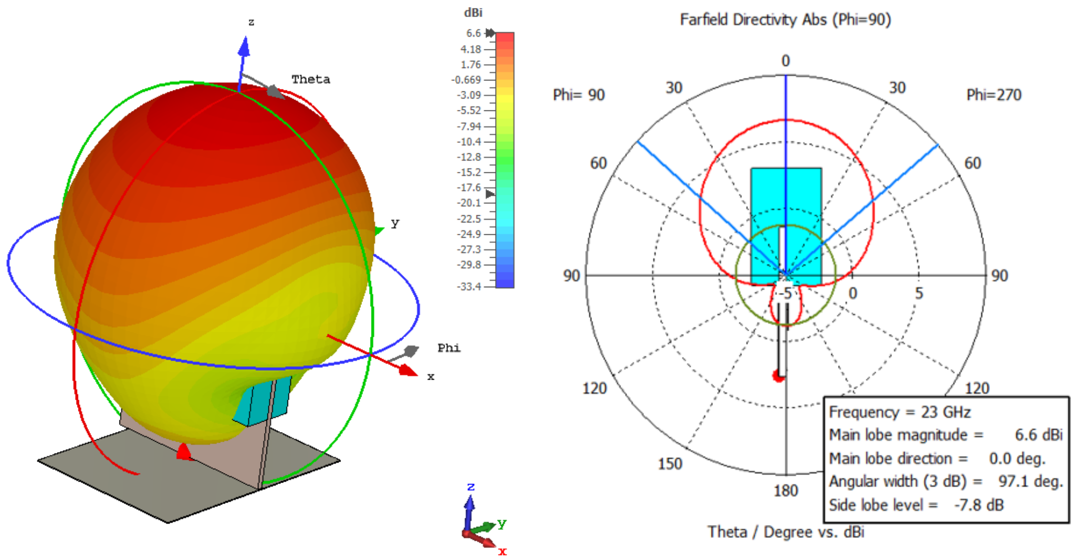

Figure 5.5: Farfield pattern of the final unit cell design

For best performance the surface current on the antenna should be uniform for whole antenna length. This means that the dimensions of the antenna are suited for the desired frequency and surface waves travel along the whole surface. The surface current is plotted on figure 5.6.

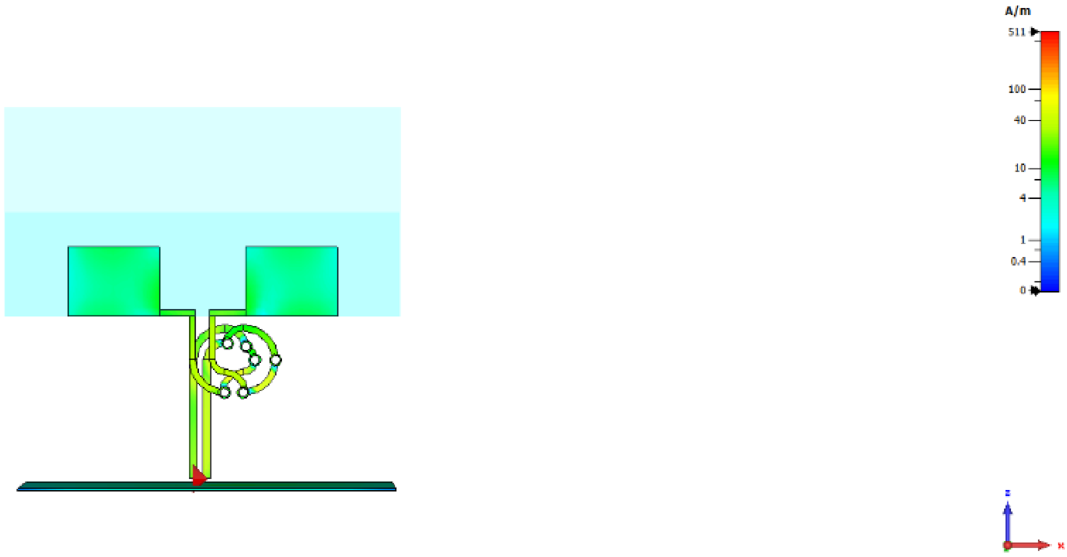

Figure 5.6: Surface current of the isolated unit cell

These results considering the radiation pattern, uniform surface current and return loss are promising and therefore this design is now simulated in an infinite array.

5.4 Final design in an infinite array

Like previously with initial design the unit cell is simulated in an infinite array with Floquet modes in an infinite array. Good results are achieved with the separation of 4.5 mm, which is 0.35λ at 23 GHz. Boundaries on the sides are unit cell boundaries, which mean that the single element is in presence of other active elements. Upper boundary is open space and lower boundary is electric wall, which represents the ground plane. The illustration of infinite array simulation is in figure 5.7.

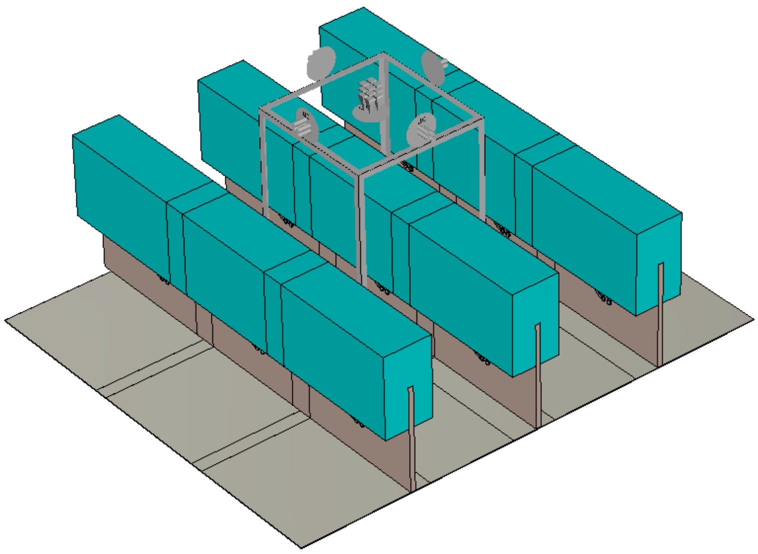

Figure 5.7: Unit in an infinite array with 0.35λ separation

The dielectrics overlap because the length of the dielectrics is larger than the antenna arms and to make the coupling between the antenna elements large the antennas must be moved very close to each other.

For this unit cell simulation also, a scanning is introduced. In figure 5.8 ϕ is azimuth and θ is elevation scan. At broadside the, ϕ=0, θ=0 the resonance frequency is 25 GHz and the bandwidth is quite narrow. This means that the unit cell still is not well impedance matched. When changing the azimuth value, the bandwidth is wider and resonance frequency shifts, because of higher impedance from the nearby elements, upwards. Elevation scan of 30 degrees is more than base stations usually have, which is 15 degrees. For elevation of 30 degrees when theta is zero the return loss increases and is higher than -10 dB in every point. The antenna has worst impedance matching at these angles. Still overall performance is not very bad since in whole band the return loss is at most bit more than -6 dB.

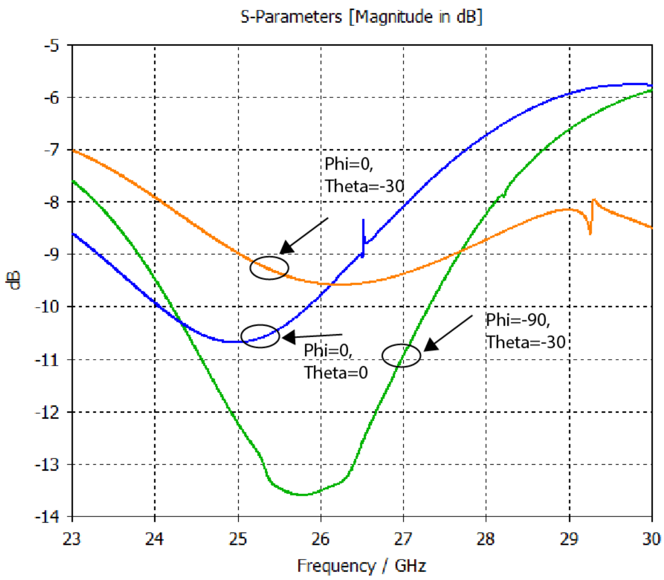

Figure 5.8: S_{11} of a unit cell in infinite array

5.5 Finite array

Unit cell in infinite array shows how the single cell radiates when in presence of other cells. In real antennas there is always an edge and the radiation is different from element to element. Therefore, to see how the whole array would radiate a full array simulation, with 484 elements is made. The elements are placed in in square, making the array 22x22 elements with the area of 99x99 mm^2, the separation in both x and y direction is the same, as before - 4.5 mm. The array is illustrated in figure 5.9, where the rectangles illustrate the dipole arms.

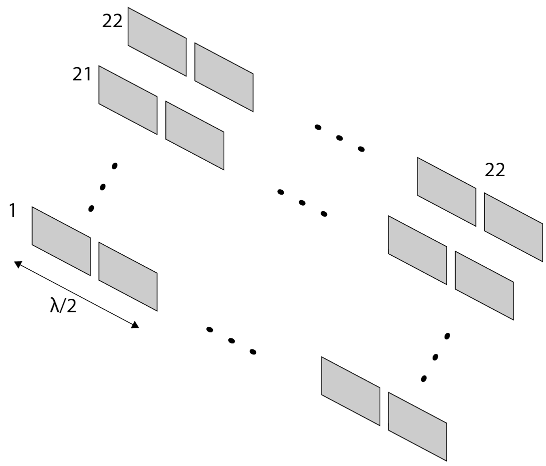

Figure 5.9: Geometry of the array

In full array simulation the return loss and gain are the main parameters which are investigated. The full array is exited simultaneously, and two edge elements and two center elements are used to plot the S_{11} values.

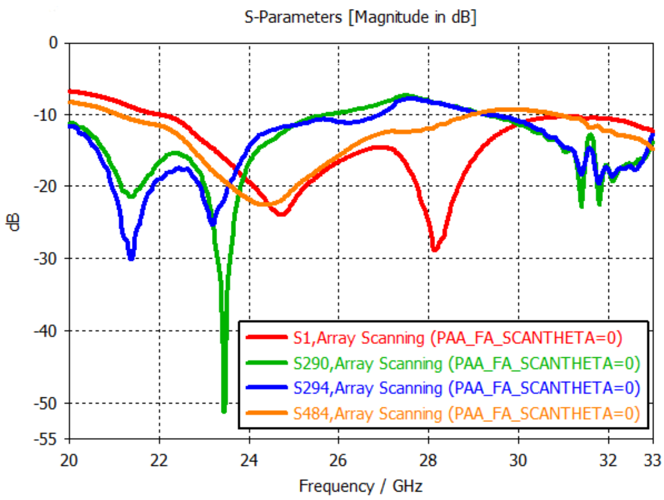

Figure 5.10: S_{11} of full array radiation in broadside

From figure 5.10 it is directly visible that the bandwidth is much larger for the full array compared to the single antenna element. Although not being under -10 dB for entire band the return loss is -8 dB at maximum around 28 GHz. From this graph two effects of mutual coupling are apparent, first the edge elements are not affected as much as center elements, because the radiation is only from one side and secondly that the bandwidth is significantly larger for connected array compared to the single antenna. This because when moving the antenna elements closer together the capacitance between the elements increases and compensates the inductance in the ground plane which in turn acts as LC circuit and oscillates. Higher frequency resonances are coupled and radiated, thus the bandwidth increases. The number of elements calculated for 30 dBi gain was quite accurate, providing 30.2 dBi gain at broadside direction. Farfield pattern for whole array is in figure 5.11.

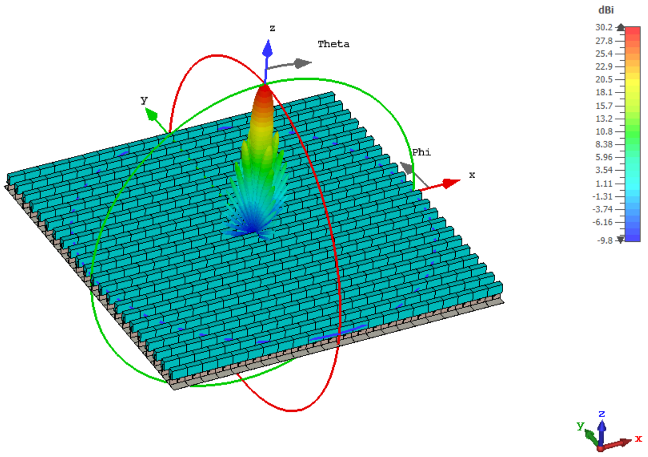

Figure 5.11: Farfield pattern of full array

Farfield in polar plot is plotted, where at 23 GHz the radiation pattern has nice distinguishable main lobe and low side lobes.

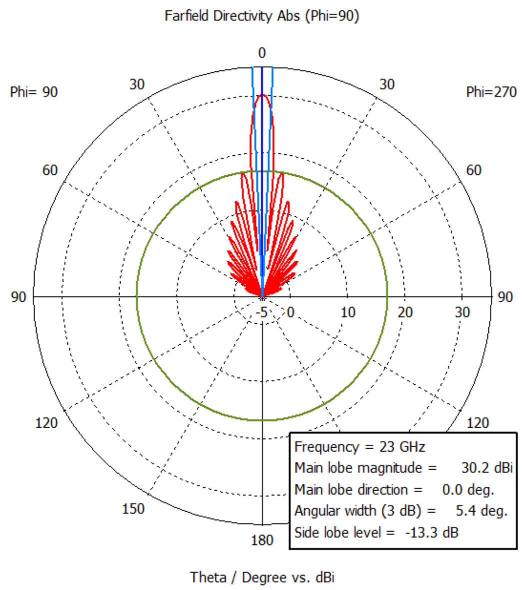

Figure 5.12: Farfield of full array in polar plot for 23 GHz

Similarly, as for unit cell the surface current is observed on the full array. It is seen that the surface current is not entirely uniform on the surface of the antenna, but the differences in current levels are not very big and the lower current regions are relatively small.

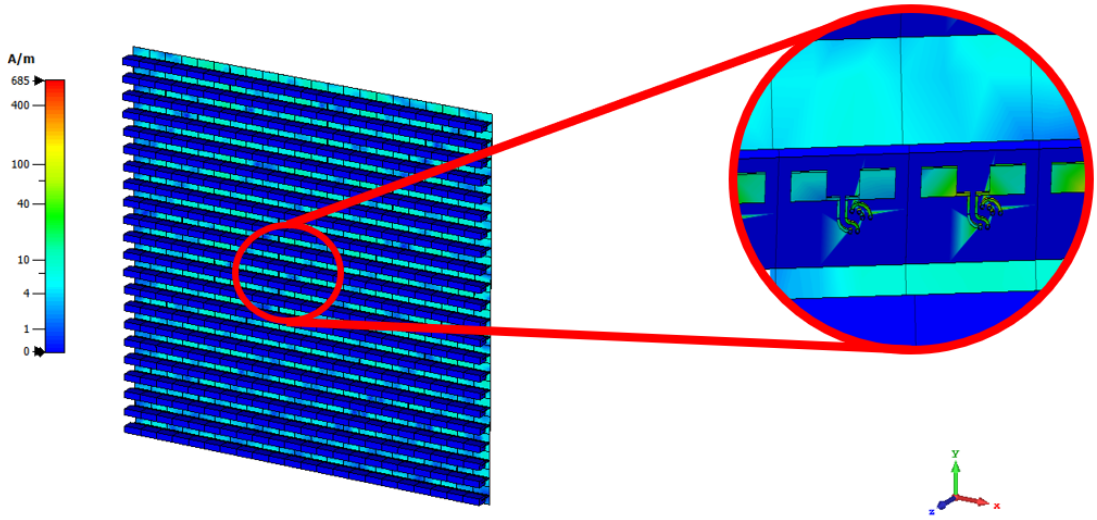

Figure 5.13: Surface current on the full array

5.6 Array scanning

Main concept and advantage with phased array antennas is the beamsteering ability. State-of-the-art antennas like presented in [3] have scanning of 45 degrees in both elevation and azimuth simultaneously. However, in this millimeter band mobile base station application scanning of at least 15 degrees is good.

Elevation is scanned from 20 to 60 degrees with 20-degree steps to see how the return loss changes. This is plotted in figure 5.14.

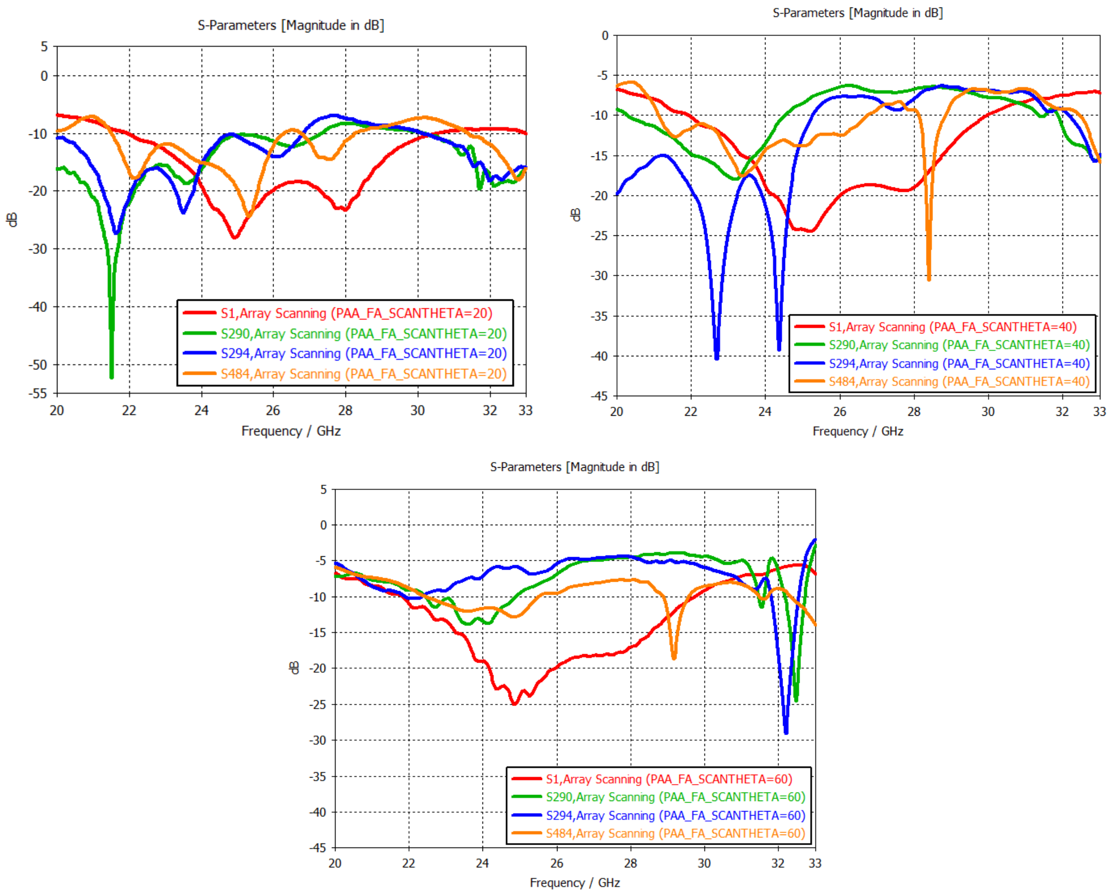

Figure 5.14: Array elevation scan for 20, 40 and 60 degrees from top left respectively

At high elevation scan angles the array performance is not good, but up to 20 degrees the return loss is still around at least -7 dB. The gain, when scanning drops by almost 3 dB, because of the higher reflection coefficient.

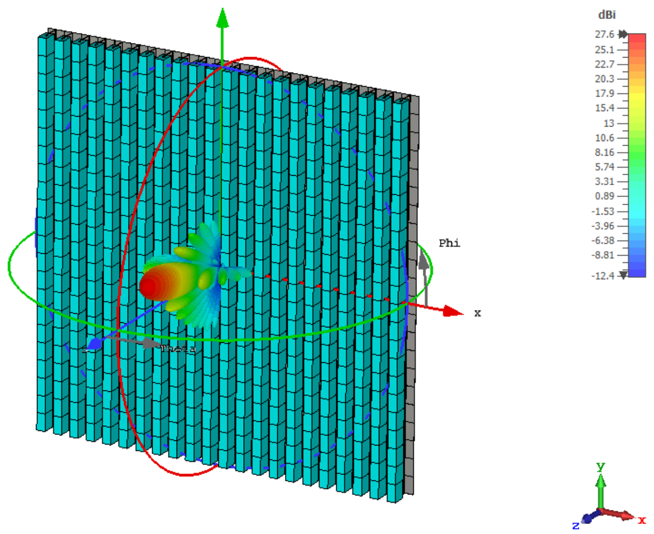

Figure 5.15: Array scanning, θ=20° ϕ=70° at 23 GHz

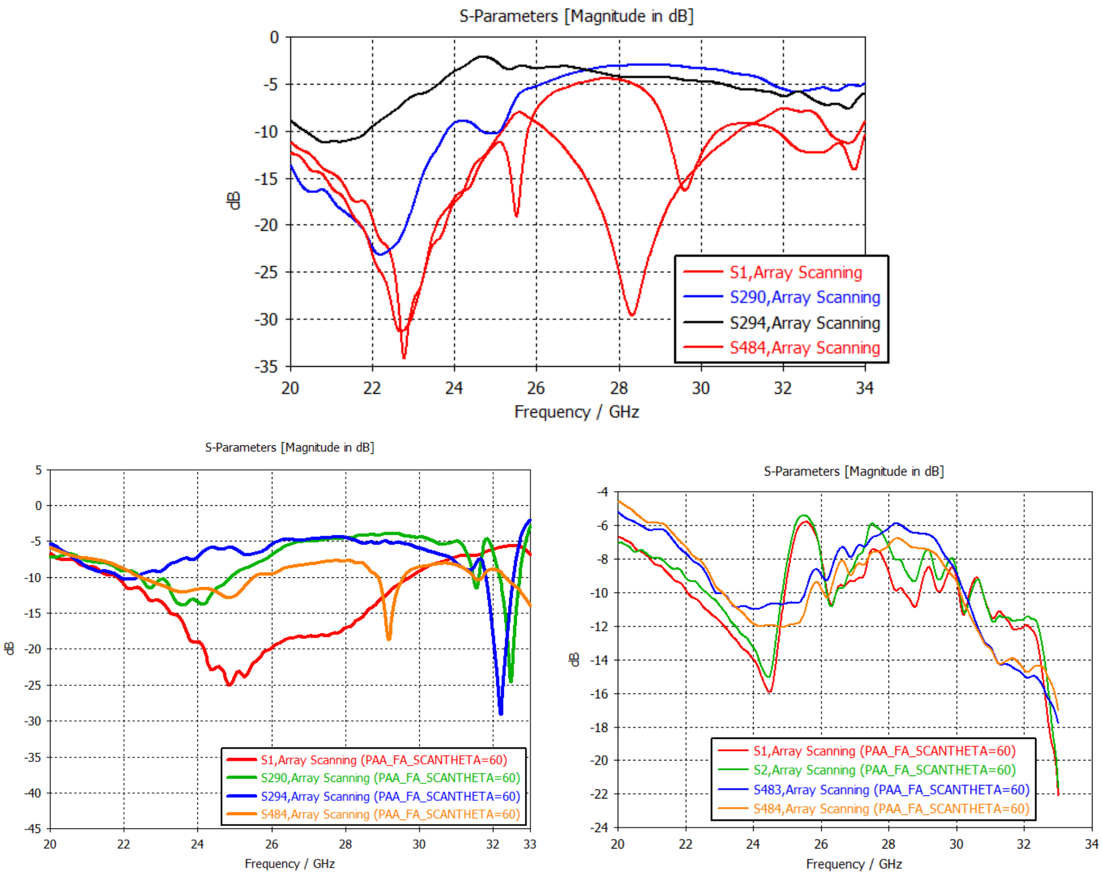

Figure 5.16: θ 60-degree elevation at 4 mm, 4.5 mm and 6.3 mm separations from top respectively

5.7 Separation

To find the optimal separation between the elements several simulations for separations from 4 mm to 6.3mm, which is $\lambda/2$ at 32 GHz are made. When the elements are overlapping at the separation of 4 mm the return loss is high and antenna is not radiating well. On the other end at large separation radiation pattern is inconsistent over wide bandwidth while at 4.5 mm separation the return loss is higher than for larger separation, but it is more uniform and by optimizing the array a bit it could be lowered. This shows that the connected antennas indeed have more uniform current distribution and wide bandwidth and scanning angle can be achieved.

6
Conclusion and further work

In this master's thesis a connected phased array antenna was designed. The design process started with an investigation of current wideband antennas and antenna arrays where several solutions were pointed out but were not suitable, mainly because of the limited scanning angle. The Vivaldi antenna for example has very wide bandwidth, but the scan range is limited to ca. $\pm$ 40 degrees. Wider scanning can be achieved with an array consisting of patch antennas, but the bandwidth is not as high as for the Vivaldi antenna.

Therefore, a connected antenna array solution is proposed in this thesis. In every antenna array there will be mutual coupling in-between the elements. This coupling creates surface waves which in turn may create high impedance regions which by scanning cause scan blindness or limit the antenna bandwidth. Traditionally the surface current is suppressed with EBG materials or by increasing the antenna separation. In this thesis however, a different solution is proposed. By moving the antenna elements very close together the mutual coupling increases and the surface current on along the array will be uniform. This means that the impedance is also uniform and then a wide scanning can be achieved since the feeding network can be matched with the array impedance.

Another advantage with the proposed solution is the wide bandwidth of the array. When the elements are closely coupled, the capacitance between the elements increases and with that higher frequencies are coupled and radiated, because the capacitance between the elements together with ground plane inductance generates oscillations, like LC circuit. Wheeler was first to propose an infinite current sheet and Munk introduced the wide band antenna array where capacitors were added between the antenna elements [42].

In this work, by increasing the capacitance by reducing the antenna separation, the goal of an array antenna with wide band performance was met. The array has a bandwidth of 37% at center frequency of 27 GHz. Similar percentage bandwidth is achieved at azimuth scanning of 70° and elevation 20° when relaxing the VSWR from 2 to 2.6. The proposed antenna array, consisting of 484 elements has a pencil-beam radiation pattern and yields a gain of 30 dBi. Therefore, the goal to propose a wide band and wide scan planar antenna array was fulfilled.

6.1 Further work

This thesis about the connected antennas is just a small more-or-less proof of concept showing that the connected arrays could be used in millimeter band 5G applications. Further work and time are needed to optimize the antenna for wider bandwidth and higher scanning angles. This could be done by performing element by element excitation array simulation to determine which elements at specific angle alter the performance. These elements could then be switched off or changed to passive ones instead.

Further improvement may be achieved by investigating the top dielectric layer. Several works propose an ADL layer on top of the antennas to increase the bandwidth. For this work a metamaterial-like surface was considered, but since the metamaterial topic by itself is very broad then considering the time limits of the thesis this solution was abandoned.

Finally, in the thesis an antenna with feeding loop is proposed, but in order to fabricate a functional antenna a feeding network and BALUN to 100 Ω must be designed as well. Since the array has many elements this is also challenging because of the frequency shifts and limitations in space.

Bibliography

[1] "Directivity - Antenna-Theory.com." [Online]. Available: http://www.antenna-theory.com/basics/directivity.php

[2] P. Bondyopadhyay, "The first application of array antenna," in *Proceedings 2000 IEEE International Conference on Phased Array Systems and Technology (Cat. No.00TH8510).* IEEE, pp. 29–32. [Online]. Available: http://ieeexplore.ieee.org/document/858903/

[3] D. Cavallo, "Connected array antennas : analysis and design," 2011. [Online]. Available: https://research.tue.nl/en/publications/connected-array-antennas-analysis-and-design

[4] D. Cavallo, W. H. Syed, and A. Neto, "6–15 GHz Wide Scanning Connected Array," in *2018 IEEE International Symposium on Antennas and Propagation & USNC/URSI National Radio Science Meeting.* IEEE, jul 2018, pp. 2155–2156. [Online]. Available: https://ieeexplore.ieee.org/document/8608367/

[5] C. Kolitsidas, "Next Generation Wideband Antenna Arrays for Communications and Radio Astrophysics," 2017. [Online]. Available: http://www.diva-portal.org/smash/record.jsf?pid=diva2:1158607

[6] "3G & 4G Frequency List – AlwaysOnline Wireless." [Online]. Available: https://support.alwaysonlinewireless.com/hc/en-us/articles/115002446723-3G-4G-Frequency-List

[7] "3G & 4G Frequency List – AlwaysOnline Wireless." [Online]. Available: https://support.alwaysonlinewireless.com/hc/en-us/articles/115002446723-3G-4G-Frequency-List

[8] M. Novak, E. Alwan, F. Miranda, and J. Volakis, "Conformal and Spectrally Agile Ultra Wideband Phased Array Antenna for Communication and Sensing," Tech. Rep. [Online]. Available: https://ntrs.nasa.gov/search.jsp?R=20150023062

[9] R. W. Kindt and W. R. Pickles, "Ultrawideband All-Metal Flared-Notch Array Radiator," *IEEE Transactions on Antennas and Propagation*, vol. 58, no. 11, pp. 3568–3575, nov 2010. [Online]. Available: http://ieeexplore.ieee.org/document/5560754/

[10] "Directivity - Antenna-Theory.com." [Online]. Available: http://www.antenna-theory.com/basics/directivity.php

[11] "On which computational technique does CST Studio Suite work?" [Online]. Available: https://www.researchgate.net/post/On{_}which{_}computational{_}technique{_}does{_}CST{_}Studio{_}Suite{_}work

[12] "Why do we use Method of Moments (MOM) techniques even though we have a well established FDTD tech-

nique?" [Online]. Available: https://www.researchgate.net/post/Why{_}do{_}we{_}use{_}Method{_}of{_}Moments{_}MOM{_}techniques{_}even{_}th

[13] Androidauthority, "5G dangers: mmWave microwaves and other health claims debunked." [Online]. Available: https://www.androidauthority.com/5g-dangers-895776/

[14] *Foundations of Antenna Engineering: A Unified Approach for Line-of-Sight and Multipath.* Artech House, 2015.

[15] "Classification of Polarization." [Online]. Available: http://hyperphysics.phy-astr.gsu.edu/hbase/phyopt/polclas.html

[16] "Classification of Polarization." [Online]. Available: http://hyperphysics.phy-astr.gsu.edu/hbase/phyopt/polclas.html

[17] "Directivity - Antenna-Theory.com." [Online]. Available: http://www.antenna-theory.com/basics/directivity.php

[18] "Directivity - Antenna-Theory.com." [Online]. Available: http://www.antenna-theory.com/basics/directivity.php

[19] C. A. Balanis, *Antenna theory: analysis and design.* John wiley & sons, 2016.

[20] "Directivity - Antenna-Theory.com." [Online]. Available: http://www.antenna-theory.com/basics/directivity.php

[21] A. El-Banna, "E-716-A Mobile Communications Systems Integrated Technical Education Cluster At AlAmeeria," Tech. Rep., 2015. [Online]. Available: http://bu.edu.eg/portal/uploads/Engineering,Shoubra/ElectricalEngineering/2461/crs-12001/Files/E-716-A{_}lec12.pdf

[22] J. L. Allen and B. Diamond, "Mutual coupling in array antennas," MASSACHUSETTS INST OF TECH LEXINGTON LINCOLN LAB, Tech. Rep., 1966.

[23] "Mutual Coupling - MATLAB & Simulink - MathWorks Nordic." [Online]. Available: https://se.mathworks.com/help/antenna/ug/mutual-coupling.html

[24] A. Emadeddin, S. Shad, Z. Rahimian, and H. Hassani, "High mutual coupling reduction between microstrip patch antennas using novel structure," *AEU - International Journal of Electronics and Communications*, vol. 71, pp. 152–156, jan 2017. [Online]. Available: https://www.sciencedirect.com/science/article/pii/S143484111630526X

[25] N. Fadlallah, M. Rammal, and P. Vaudon, "Effects of mutual coupling in phased arrays with buttler network feed," in *17th International Conference on Applied Electromagnetics and Communications, 2003. ICECom 2003.* IEEE, pp. 374–379. [Online]. Available: http://ieeexplore.ieee.org/document/1291030/

[26] R. Garg, *Microstrip antenna design handbook.* Artech House, 2001.

[27] "CHAPTER-6 SCAN BLINDNESS IN PHASED ARRAY AND ITS ELIMINATION," Tech. Rep. [Online]. Available: http://shodhganga.inflibnet.ac.in/bitstream/10603/187153/14/14_chapter6.pdf

[28] G. Donzelli, F. Capolino, S. Boscolo, and M. Midrio, "Elimination of Scan Blindness in Phased Array Antennas Using a Grounded-Dielectric EBG Material," *IEEE Antennas and Wireless Propagation Letters*, vol. 6, pp. 106–109, 2007. [Online]. Available: http://ieeexplore.ieee.org/document/4142731/

[29] Pasternack.com, "Microstrip Patch Antenna Calculator." [Online]. Available: https://www.pasternack.com/t-calculator-microstrip-ant.aspx

[30] M. Civerolo and D. Arakaki, “Aperture coupled patch antenna design methods,” in *2011 IEEE International Symposium on Antennas and Propagation (APSURSI).* IEEE, jul 2011, pp. 876–879. [Online]. Available: http://ieeexplore.ieee.org/document/5996415/

[31] D. Pozar, “Microstrip antenna aperture-coupled to a microstripline,” *Electronics Letters*, vol. 21, no. 2, p. 49, 1985. [Online]. Available: https://digital-library.theiet.org/content/journals/10.1049/el_19850034

[32] G. Kumar, “Dipole Antennas,” Tech. Rep. [Online]. Available: https://nptel.ac.in/courses/108101092/Week-2-DipoleAntenna.pdf

[33] “Microstrip Calculator.” [Online]. Available: https://www.pasternack.com/t-calculator-microstrip.aspx

[34] D. M. Pozar, *Microwave engineering.* John Wiley & Sons, 2009.

[35] “Impedance Matching - Taper Transformer.” [Online]. Available: http://www.amanogawa.com/archive/Taper/Taper-2.html

[36] “What is the difference between common mode and differential mode? | FAQ | TDK Product Center.” [Online]. Available: https://product.tdk.com/info/en/contact/faq/faq_detail_D/1432758486037.html

[37] M. Y. Algumaei, N. A. Shairi, Z. Zakaria, and I. M. Ibrahim, “Review of Mixer and Balun Designs for UWB Applications,” Tech. Rep., 2017. [Online]. Available: http://www.ripublication.com

[38] Optiprint-AG, “Optiprint Technical Information,” Optiprint AG, Berneck, Tech. Rep., 2012. [Online]. Available: http://www.optiprint.ch

[39] “Minimum Drill Size and Drill Requirements - Bittele.” [Online]. Available: https://www.7pcb.com/blog/dimensions-drills-highest-lowest-diameter.php

[40] “Bow Tie Antennas.” [Online]. Available: http://www.antenna-theory.com/antennas/wideband/bowtie.php

[41] M. K. A. Rahim, M. Z. A. Abdul Aziz, and C. S. Goh, “Bow-Tie Microstrip Antenna Design,” in *2005 13th IEEE International Conference on Networks Jointly held with the 2005 IEEE 7th Malaysia International Conf on Communic*, vol. 1. IEEE, pp. 17–20. [Online]. Available: http://ieeexplore.ieee.org/document/1635425/

[42] I. Tzanidis, J. P. Doane, K. Sertel, and J. L. Volakis, “Wheeler’s current sheet concept and Munk’s wideband arrays,” in *Proceedings of the 2012 IEEE International Symposium on Antennas and Propagation.* IEEE, jul 2012, pp. 1–2. [Online]. Available: http://ieeexplore.ieee.org/document/6349119/